Table 2
Postoperative high–dose rate brachytherapy for soft tissue sarcomas

Characteristics	Number
Interval between OP and BT (days)	
Mean	5.3 (range, 1–7)
<5	2
>5	24
Median number of applicators	7 (range, 2–15)
Fractional dose	
4.5 Gy	1
6 Gy	25
Number of fractions	
5	1
6	25
Total dose (EQD2 for tumor control)	
27 Gy (32.6 Gy)	1
30 Gy (40 Gy)	1
36 Gy (48 Gy)	24
Mean volume encircled by the prescribed dose	74.9 cc (range, 18.5–173)

OP = operation; BT = brachytherapy; EQD2 = equivalent dose with 2 Gy fraction.

between the operation and the HDRBT was 5.3 days in a mean, and 24 HDRBTs were commenced between 5 and 7 days after the operation. Number of implanted tube applicators ranged from two to 15 with a median of seven. The treated volume encircled by the prescribed dose ranged from 18.5 to 173 cc with a mean of 74.9 cc. Chemotherapy was delivered in 12 lesions.

Median followup length was 49.7 months ranging from 4.7 to 187 months. Local recurrence-free survival (LRFS) was calculated in the 26 lesions, and overall survival (OS) in all the 25 patients. Local recurrence was defined as a regrowth of the STS within 5 cm from the operation scars. LRFS and OS were calculated by Kaplan–Meier method (11) with a difference between the survival curves evaluated by a logrank test. Acute morbidities seen within 6 months after HDRBT were classified according to the National Cancer Institute Common Terminology Criteria for Adverse Events version 3.0, whereas Radiation Therapy Oncology Group/European Organization for Research and Treatment for Cancer criteria were used for late morbidities (12).

Results

Local recurrence was observed in five lesions. All the local recurrences occurred outside of the treated volume of HDRBT. These local recurrences were within the treated volume, if postoperative EBRT were administered encompassing all the surgical scars with 5 cm margins. LRFS of all 26 lesions was 78.2% in 5 years. According to the surgical margin status, 5-year LRFSs of positive and negative margins were 90.9% and 64.6%, respectively, without

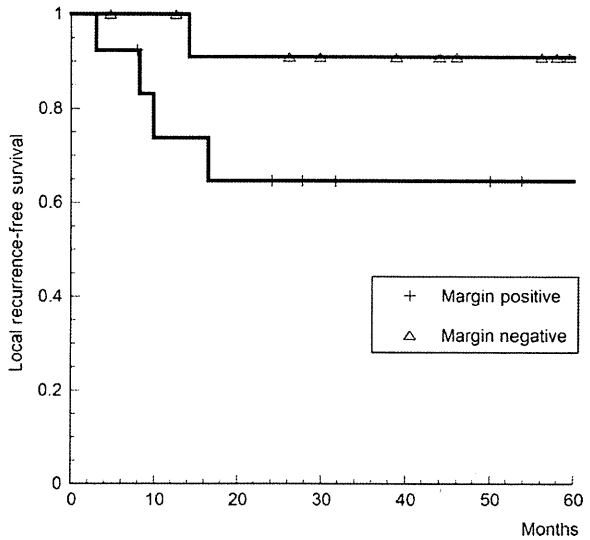

Fig. 1. Local recurrence-free survivals according to surgical margin status.

a statistically significant difference ($p = 0.11$) (Fig. 1). In the lesions treated as a primary therapy, LRFS is 90.9% in 5 years, whereas the recurrent lesions after previous operations showed 5-year LRFS rate of 66.5% ($p = 0.15$) (Fig. 2). The lesions were classified into two groups according to the surgical margin status and number of foregoing operations. Group 1 was defined as recurrent lesions, which were resected with positive surgical margins. All other lesions were classified into Group 2. There were eight lesions in Group 1 and 18 in Group 2. Five-year LRFS was 43.8% and 93.3% in Group 1 and Group 2, respectively

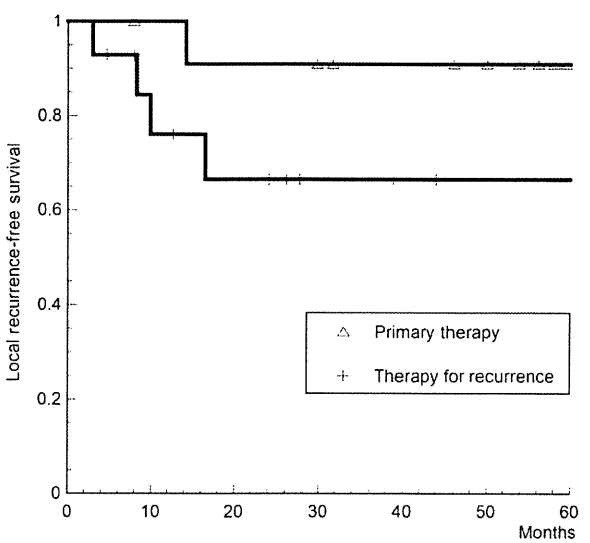

Fig. 2. Local recurrence-free survivals according to number of previous operations.

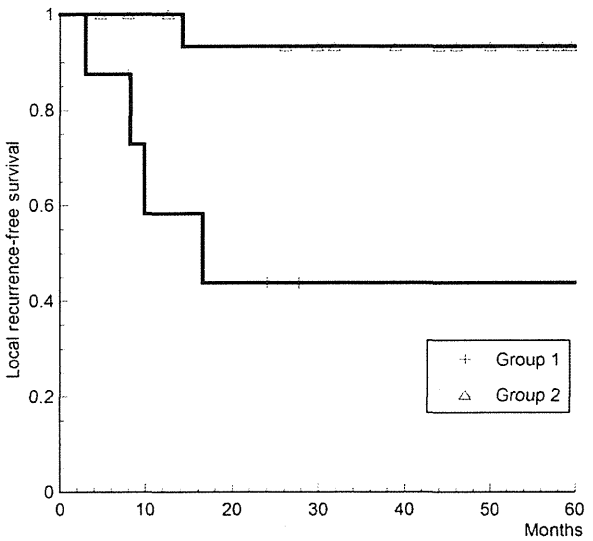

Fig. 3. Local recurrence-free survivals according to the group classification by surgical margin status and number of previous operations (for details refer to the text).

(Fig. 3). The difference reached a statistical significance with $p = 0.004$. Sex, malignant grade, tumor size, number of applicators, and treated volume were found to have no statistically significant influences on LRFS. In the 23 lesions of the extremity STSs, only one amputation was required to control recurrence.

OS of 25 patients was 75.6% in 5 years. There were only 2 patients with Grade 1 malignancy and both of them were alive without recurrence. The patients with Grade 2 and 3 lesions showed similar OSs and 71.6% of them were alive for 5 years.

Acute morbidities were seen in 7 patients with Grade 1 morbidities in 6 patients and Grade 2 in 1 patient (Table 3). Grade 1 morbidities were a slight bleeding from the scar at the time of applicator removal, slight erosion of skin, and seroma formation requiring aspiration only once or twice. Grade 2 morbidity was wound dehiscence, which healed with conservative measures. Chronic morbidities were seen in 4 patients. The Grade 3 and 4 morbidity were seen each in 1 patient. Grade 4 morbidity was bone exposure at the HDRBT site requiring surgical removal of the sequester and repair with bone transplantation. The Grade 3 morbidity was fistula formation with an ensuing infection managed by debridement. Both morbidities occurred within 24 months after HDRBT. Five-year rate of chronic morbidities equal to or greater than Grade 2 was 14.6%.

Table 3
Number of morbidities of postoperative high–dose rate brachytherapy

Morbidities	Morbidity grade	Number of morbidities
Acute morbidity		
Wound complication	1	4
	2	2
Paresthesia	1	1
Seroma formation	1	1
Late morbidity		
Wound complication	2	1
Seroma formation	1	1
Bone exposure	4	1
Infectious fistula	3	1

Discussions

In the management of STS, limb-sparing operation with perioperative radiation therapy has been established as a standard (13). With that combination, LRFS rate is reported to be 75–100% (1–4, 14). However, local recurrence rate is strongly influenced by the surgical margin status, number of previous operations, grade of malignancy, and primary site of STS (1, 2). In the present study, operative margins were microscopically positive in 50% of the patients and the remaining patients had very close margins less than 5 mm. Furthermore, 54% of the lesions were classified as Grade 3 malignancies. Considering the adverse features of this series, LRFS rate of 78.2% in 5 years is relatively favorable. The marginal status, number of the previous operations, and the grade of malignancy did not have an influence on LRFS with a statistical significance, probably because of the small number of the patients in this series. However, the recurrent lesions resected with positive surgical margins showed a poor 5-year LRFS of 43.8% in comparison to the other lesions with 93.3% LRFS in 5 years.

Brachytherapy has an advantage of concentrating dose distribution onto the tumor region with a simultaneous sparing of normal tissues (15), whereas EBRT with wide fields encompassing tumor as well as surgical beds sometimes causes bone fracture, subcutaneous fibrosis, and lymphedema distal to the irradiated site (16). According to Memorial Sloan-Kettering Cancer Center studies, postoperative LDRBT as a single modality reduces local recurrence in margin-negative high-grade STS (1, 3). The LDRBT did not include operative scars and drainage scars in the treated volume. In contrary, local recurrence was not reduced by LDRBT alone in postoperative low-grade STSs (17). They also suggested that high-grade STSs with positive surgical margins are better treated by combination of EBRT and LDRBT (5). Although HDRBT has advantages that radiation dose distribution can be optimized by the manipulation of dwell positions and dwell times of ^{192}Ir source, and radiation exposure to the medical personnel is negligible, the paucity of reported series makes it difficult to establish the optimal fractionation and total dose of HDRBT (6–10). Retrospective analyses revealed that combined EBRT and HDRBT is well tolerated and reduce local recurrence. Chun *et al.* (6) showed that local recurrence was not seen in 17 patients treated with 12–18 Gy

of 6 fractions of HDRBT combined with EBRT of 36–60 Gy. Pohar *et al.* (9) demonstrated that 2-year local control of 94% could be obtained with HDRBT of 13.5 Gy in three fractions with EBRT. Koizumi *et al.* (7) showed somehow poorer local control rate of 48% in 2 years because of the adverse features of their patients with macroscopic residual disease in 31%. In the present study, HDRBT was used without EBRT. HDRBT was delivered to the tumor bed without including surgical and drainage scars. At the launch of the postoperative HDRBT, radiation was planned to be confined to the tumor bed based on the reports from Memorial Sloan-Kettering Cancer Center. Because most of the patients in this series underwent resections reaching to the major neurovascular bundles and the high-dose radiation to them could cause serious morbidities, the total dose of HDRBT was determined by tolerance dose of peripheral nerve assumed as about 60 Gy in a conventional fractionation. The corresponding biologically equivalent dose by 2 Gy fractionation was calculated by linear quadratic model assuming $\alpha/\beta = 10$ Gy and 3 Gy for tumor control and late toxicity, including nerve damage, respectively (18). The equivalent dose by 2 Gy fractionation for HDRBT of 36 Gy was 48 Gy and 64.8 Gy, respectively, for tumor control and late toxicity. Because of the favorable results, this field setup and fractionation regimen of HDRBT have been continued to the present time.

Despite the retrospective nature of this study and the small number of patients, HDRBT alone with the fractionation regimens used in this study seems to be satisfactory to sterilize lesions in the treated volume. However, poor LRFS of 43.8% in 5 years demonstrates that in lesions treated for recurrence and whose surgical margins are positive, STSs tended to recur outside of the treated volume of HDRBT but within 5 cm from the surgical scars. It seems that they had better been treated with combination of HDRBT and wide field EBRT encompassing surgical beds as well as scars and drainage sites.

Serious late morbidity was seen in 2 patients, both of which could be repaired by surgical procedures. Although it is recommended to begin brachytherapy no sooner than 5 days after the operation (1, 15), 2 patients irradiated with a shorter interval did not have any serious morbidities. There were no patients who underwent limb amputation because of morbidities.

Conclusions

In summary, HDRBT alone to the tumor bed without including surgical scars and drainage sites with 36 Gy/6 fractions/3 d seems to be adequate and tolerable as a postoperative treatment for patients initially operated and/or negative for surgical margins. If the lesion is operated for recurrence and surgical margins are positive, administration of wide fields EBRT is recommended.

Acknowledgment

This work was partly supported by Grant-in-Aid for Cancer Research from the Ministry of Health, Labor, and Welfare, Japan.

References

[1] Pisters PWT, Leung DHY, Woodruff J, *et al.* Analysis of prognostic factors in 1041 patients with localized soft tissue sarcomas of the extremities. *J Clin Oncol* 1996;14:1679–1689.
[2] Zagars GK, Ballo MT, Pisters PWT, *et al.* Preoperative vs. postoperative radiation therapy for soft tissue sarcoma: A retrospective comparative evaluation of disease outcome. *Int J Radiat Oncol Biol Phys* 2003;56:482–488.
[3] Pisters PWT, Harrison LB, Leung DHY, *et al.* Long-term results of a prospective randomized trial of adjuvant brachytherapy in soft tissue sarcoma. *J Clin Oncol* 1996;14:859–868.
[4] Yang JC, Chang AE, Baker AR, *et al.* Randomized prospective study of the benefit of adjuvant radiation therapy in the treatment of soft tissue sarcomas of the extremity. *J Clin Oncol* 1998;16:197–203.
[5] Alekhteyar KM, Leung DH, Brennan MF, *et al.* The effect of combined external beam radiotherapy and brachytherapy on local control and wound complications in patients with high-grade soft tissue sarcomas of the extremity with positive microscopic margin. *Int J Radiat Oncol Biol Phys* 1996;36:321–324.
[6] Chun M, Kang S, Kim BS, *et al.* High dose rate interstitial brachytherapy in soft tissue sarcoma: Technical aspects and results. *Jpn J Clin Oncol* 2001;31:279–283.
[7] Koizumi M, Inoue T, Yamazaki H, *et al.* Perioperative fractionated high-dose rate brachytherapy for malignant bone and soft tissue tumors. *Int J Radiat Oncol Biol Phys* 1999;43:989–993.
[8] Martinez-Monge R, San Julian M, Amillo S, *et al.* Perioperative high-dose-rate brachytherapy in soft tissue sarcomas of the extremity and superficial trunk in adults: Initial results of a pilot study. *Brachytherapy* 2005;4:264–270.
[9] Pohar S, Haq R, Liu L, *et al.* Adjuvant high-dose-rate and low-dose-rate brachytherapy with external beam radiation in soft tissue sarcoma: A comparison of outcomes. *Brachytherapy* 2007;6:53–57.
[10] Nag S, Porter AT, Donath D. The role of high dose rate brachytherapy in the management of adult soft tissue sarcomas. In: Nag S, editor. *High dose rate brachytherapy. A textbook.* New York, NY: Futura Publishing Company; 1994. p. 393–408.
[11] Kaplan EL, Meier P. Nonparametric estimation from incomplete observations. *J Am Stat Assoc* 1958;53:457–481.
[12] Perez CA, Brady LW. Principles and practice of radiation oncology. Philadelphia, PA: JB Lipppincot Company; 1993. pp. 53–55.
[13] Pisters PWT, O'Sullivan B, Maki RG. Evidence-based recommendations for local therapy for soft tissue sarcomas. *J Clin Oncol* 2007;25:1003–1008.
[14] Suit HD, Mankin HJ, Wood WC, *et al.* Treatment of the patient with stage M0 soft tissue sarcoma. *J Clin Oncol* 1988;6:854–862.
[15] Nag S, Shasha D, Janjan N, *et al.*, American Brachytherapy Society. The American Brachytherapy Society recommendations for brachytherapy of soft tissue sarcomas. *Int J Radiat Oncol Biol Phys* 2001;49:1033–1043.
[16] Davis AM, O'Sullivan B, Turcotte R, *et al.*, Canadian Sarcoma GroupNCI Canada Clinical Trial Group Randomized Trial. Late radiation morbidity following randomization to preoperative versus postoperative radiotherapy in extremity soft tissue sarcoma. *Radiother Oncol* 2005;75:48–53.
[17] Pisters PWT, Harrison LB, Woodruff JM, *et al.* A prospective randomized trial of adjuvant brachytherapy in the management of low-grade soft tissue sarcomas of the extremity and superficial trunk. *J Clin Oncol* 1994;12:1150–1155.
[18] Fowler JF. The linear-quadratic formula and progress in fractionated radiotherapy. *Br J Radiol* 1989;62:679–694.

Results of T4 Surgical Cases in the Japanese Lung Cancer Registry Study

Should Mediastinal Fat Tissue Invasion Really be Included in the T4 Category?

Shun-ichi Watanabe, MD, Hisao Asamura, MD,* Etsuo Miyaoka, PhD,† Meinoshin Okumura, MD,‡ Ichiro Yoshino, MD,§ Yoshitaka Fujii, MD,‖ Yoichi Nakanishi, MD,¶ Kenji Eguchi, MD,# Masaki Mori, MD,** Noriyoshi Sawabata, MD,‡ and Kohei Yokoi, MD,† for the Japanese Joint Committee of Lung Cancer Registry*

Introduction: T4 lung cancer is a heterogeneous group of locally advanced disease. We hypothesized that patients in whom T4 lung cancer invaded only mediastinal fat tissue would show better prognosis after surgery than patients in whom T4 disease invaded other organs. The present study aimed to investigate how different invasive features of T4 disease impacted prognosis, and what types of patients with T4 disease could benefit most from surgical treatment.

Methods: A nationwide registry study on lung cancer surgical cases during 2004 was conducted by the Japanese Joint Committee of Lung Cancer Registry, including registries of 11,663 cases within Japan. The present study analyzed 215 of these cases involving T4 structures or with ipsilateral nonprimary lobe pulmonary metastasis (PM).

Results: Reasons for T4 classification included invasion of only mediastinal tissue in 32 cases (15%), invasion of other structures in 96 cases (45%), and ipsilateral different lobe PM in 87 cases (40%); among these three groups, there were no significant differences in survival, nodal status, and patterns of first recurrence. Multivariate analysis showed an age of 70 years or above ($p = 0.022$) and nodal status ($p = 0.004$) to be significant prognostic factors. T4N0 patients less than 70 years of age showed significantly better prognosis than those who were T4N1–2 and 70 years of age or older ($p = 0.0001$; 5-year survival rate 50.3 versus 19.9%).

Conclusions: There was no significant difference in survival between T4 patients with only mediastinal fat invasion and those with other T4 organ invasion and ipsilateral different lobe PM, demonstrating appropriateness of the T4 category definition in the current tumor, node, metastasis staging system. Age and nodal status were significant independent prognostic factors in T4 patients, and the best surgical candidates were shown to be T4N0 patients who were less than 70 years of age and had a 5-year survival rate of more than 50%.

Key Words: T4 lung cancer, Mediastinal tissue, Pulmonary metastasis.

(*J Thorac Oncol.* 2013;8: 759-765)

The T4 category of lung cancer is defined by invasion of the heart, mediastinal fat tissue, great vessels, trachea, recurrent laryngeal nerve, esophagus, vertebral body and carina, and additional nodules in ipsilateral different lobes.[1] In T4 cases, mediastinal fat tissue invasion is considered to be the last step before involving other mediastinal organs, such as the great vessels, esophagus, or trachea (Fig. 1).

We hypothesized that patients in whom T4 lung cancer invaded only mediastinal fat tissue would show better prognosis after surgery than those in whom T4 lung cancer invaded other organs. In the present study, we analyzed the outcomes of patients enrolled in the Japanese Lung Cancer Registry Study, who had T4 disease and underwent surgery. We also investigated whether surgery conferred different survival benefits on different types of T4 lung cancer cases.

PATIENTS AND METHODS

In 2010, the Japanese Joint Committee of Lung Cancer Registry conducted a nationwide retrospective registry study on surgical cases of primary lung cancer that had occurred during 2004. The study included registries of 11,663 cases from 253 teaching hospitals in Japan; each registry contained the previously described clinicopathologic profiles and

*Division of Thoracic Surgery, National Cancer Center Hospital, Tokyo; †Department of Mathematics, Science University of Tokyo, Tokyo; ‡Department of General Thoracic Surgery, Osaka University Graduate School of Medicine, Osaka; §Department of General Thoracic Surgery, Chiba University Graduate School of Medicine, Chiba; ‖Department of Oncology, Immunology and Surgery, Nagoya City University Graduate School of Medical Science and Medical School, Nagoya; ¶Department of Clinical Medicine, Research Institute for Diseases of the Chest, Faculty of Medical Sciences, Kyushu University, Fukuoka; #Department of Medical Oncology, Teikyo University School of Medicine, Tokyo; **Department of Pulmonary Medicine, Sapporo-Kosei General Hospital, Hokkaido; and ††Department of Thoracic Surgery, Nagoya University Graduate School of Medicine, Nagoya, Japan.

Disclosure: The authors declare no conflict of interest.

Address for correspondence: Shun-ichi Watanabe, M.D., Division of Thoracic Surgery, National Cancer Center Hospital, Tsukiji 5-1-1, Tokyo 104-0045, Japan. E-mail: syuwatan@ncc.go.jp

ISSN: 1556-0864/13/0806-0759

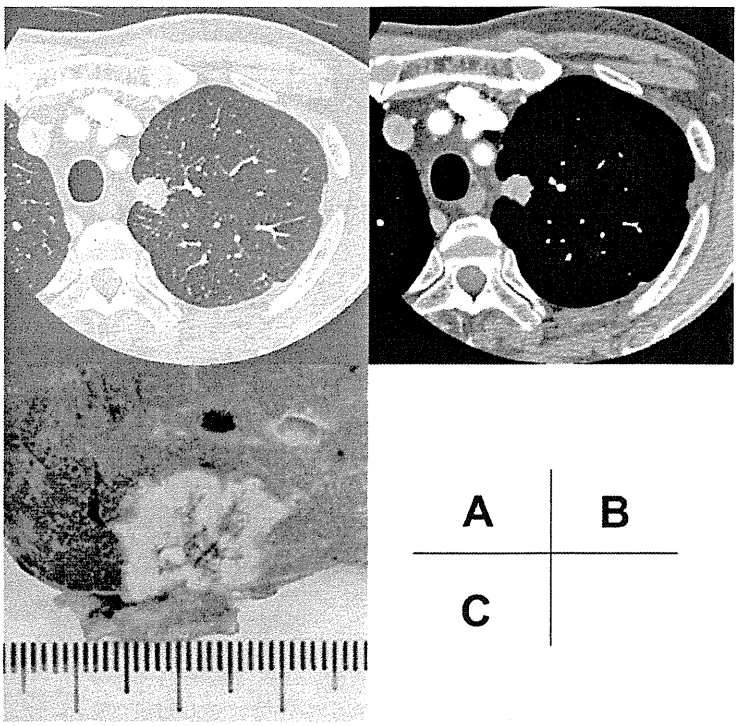

FIGURE 1. A case of pT4 disease invading the mediastinal fat tissue. *A*, CT scan (lung field window) showing a left upper lobe tumor with visceral pleura involvement. *B*, CT scan (mediastinal window) showing the tumor invading the mediastinal fat tissue. *C*, Photograph of the formalin-fixed resected specimen. CT, computed tomography.

prognoses.[2] The information collected about each tumor node metastasis (TNM) classification was used to reclassify each case according to the 7th edition of the International Union Against Cancer tumor, node, metastasis (TNM) staging system published in 2009.[1]

Of these cases, there were 218 surgical cases involving the neighboring T4 structures or ipsilateral nonprimary lobe pulmonary metastasis (PM). For the present study, three cases were excluded because the patients had both neighboring organ invasion and PM. The remaining 215 surgical cases were used in the present analysis.

Statistical Analysis

Survival was calculated by the Kaplan–Meier method, and differences in survival were determined by the log-rank test. Time zero was the date of surgery, and the terminal events were death because of cancer, noncancer, or unknown causes. Both univariate and multivariate analyses of prognostic factors were carried out using Cox proportional hazards regression models. Hazard ratios (HRs) and 95% confidence intervals were calculated. A p value less than 0.05 was considered to be statistically significant.

RESULTS

Patient Characteristics

Table 1 shows characteristics of the 215 patients enrolled in the study. The patients consisted of 166 men (77%) and 49 women (23%), with a mean age of 65.2 years and a mean tumor size of 4.5 cm. The reasons for T4 disease classification included neighboring organ invasion in 128 patients (60%) and ipsilateral different lobe PM in 87 patients (40%). Among the 128 patients with T4 disease invading neighboring organs, 32 cases (25%) invaded only mediastinal fat tissue and 96 (75%) invaded other anatomical structures. Six patients with T4 disease invading both mediastinal fat tissue and other structures were classified as other organs invasion group. The tumor cell types were adenocarcinoma in 99 (46%), squamous cell carcinoma in 77 (36%), and others in 39 patients (18%). R status was R0 in 123 (57%), R1 in 24 (11%), and R2 in 58 patients (27%). Pathologic N status was N0 in 107 (50%), N1 in 25 (12%), N2 in 79 (37%), and N3 in four patients (2%).

N and R Status Grouped by Reasons for T4 Category

Table 2 shows pathologic N status grouped by involved T4 organs. There were no significant differences in N status among the three groups ($p = 0.537$). Table 3 demonstrates R status grouped by involved T4 organs. Mediastinal fat invasion group showed significantly higher incidence of R0 than the other two groups ($p = 0.017$).

Univariate and Multivariate Analyses of Prognostic Factors

Univariate and multivariate analyses of prognostic factors were performed by means of Cox proportional hazard regression models. Univariate analysis showed age ($p = 0.02$), tumor size ($p = 0.007$), and pathologic nodal status ($p = 0.004$) to be significant prognostic factors; however, the reason for T4 disease was not a significant prognostic factor ($p = 0.949$) (Table 4). Multivariate analysis showed that ages 70 years and

TABLE 1. Patient Characteristics in Surgical Cases with Pathological T4 Disease in Japanese Lung Cancer Registry Study

No. of patients	215
Sex	
Male	166 (77%)
Female	49 (23%)
Age (yr)	
Range	32–84
Mean ± SD	65.2±10.4
Tumor size (cm)	
Range	0–15
Mean ± SD	4.5±2.4
Reasons for T4 disease	
Neighboring organ invasion	128 (60%)
Invading only mediastinal fat	32 (15%)
Invading other structures	96 (45%)
Great vessels	58
Heart	21
Esophagus	8
Vertebra	6
Carina	5
Trachea	3
Recurrent nerve	2
Ipsilateral different lobe PM	87 (40%)
Histological subtype	
Adenocarcinoma	99 (46%)
Squamous cell carcinoma	77 (36%)
Others	39 (18%)
R status	
R0	123 (57%)
R1	24 (11%)
R2	58 (27%)
RX (unclassified)	10 (5%)
Pathological nodal status	
N0	107 (50%)
N1	25 (12%)
N2	79 (37%)
N3	4 (2%)

PM, pulmonary metastasis; SD, standard deviation.

TABLE 2. N Status by Reasons for T4 Category

Reasons for T4	No. of Patients	N Status N0 (%)	N1 (%)	N2 (%)	p
Mediastinal fat invasion	31	18 (58)	4 (13)	9 (29)	0.537
Other organs invasion	95	44 (46)	14 (15)	37 (39)	—
Ipsilateral different lobe PM	85	45 (53)	7 (8)	33 (39)	—
Total	211	107 (51)	25 (12)	79 (37)	—

PM, pulmonary metastasis.

TABLE 3. R status by Reasons for T4 category

Reasons for T4	No. of Patients	R Status R0 (%)	R1 (%)	R2 (%)	p
Mediastinal fat invasion	32	26 (81)	2 (6)	4 (13)	0.017
Other organs invasion	94	47 (50)	16 (17)	31 (33)	
Ipsilateral different lobe PM	79	50 (63)	6 (8)	23 (29)	
Total	205	123 (60)	24 (12)	58 (28)	

PM, pulmonary metastasis

TABLE 4. Univariate Analysis of Prognostic Factors Using Cox Proportional Hazards Regression Models

Factors	Hazard Ratio	95% CI	p
Age (per yr increase)	1.022	1.003–1.041	0.020
Sex			
Male	1.000	—	—
Female	0.675	0.441–1.032	0.069
Tumor size (per cm increase)	1.753	1.164–2.640	0.007
Reasons for T4 disease			0.949
Mediastinal fat invasion	1.000	—	—
Other organs invasion	0.980	0.581–1.653	0.939
Ipsilateral different lobe PM	1.042	0.619–1.753	0.877
Cell type			
Non-Sq	1.000	—	—
Sq	1.138	0.792–1.636	0.484
Pathological nodal status			0.004
N0	1.000	—	—
N1	1.561	0.890–2.739	0.121
N2	1.890	1.297–2.754	0.001

CI, confidence interval; Sq, squamous cell carcinoma; PM, pulmonary metastasis.

above (p = 0.022; HR = 1.516) and pathologic nodal status (p = 0.004; HR for N0 versus N1: 1.362; HR for N0 versus N2: 1.906) were significant prognostic factors (Table 5).

Survival Analysis

Figure 2 shows the overall survival curves of the 11,663 surgical cases in the Japanese Lung Cancer Registry Study grouped by pT factors. The 3- and 5-year overall survival rates of patients with T4 disease after surgery were 48.3% and 34.5%, respectively. Figure 3 presents survival curves grouped by three reasons for T4 category (invasion of mediastinal fat, invasion of other structures, and ipsilateral different lobe PM); the 5-year survival rates in these groups were 36.1%, 36.2%, and 33.0%, respectively, with no significant between-group differences in survival. The 30-day mortality was 0.47% (1 of 215).

Table 6 describes types of first recurrence grouped by three reasons for T4 category. There was no significant difference in patterns of first recurrence among the three groups (p = 0.487).

Figure 4 shows survival curves grouped by pathologic nodal status; the 5-year survival rates in pN0, pN1, and pN2

TABLE 5. Multivariate Analysis of Prognostic Factors Using Cox Proportional Hazards Regression Models

Factors	Hazard Ratio	95% CI	*p*
Age (yr)			
<70	1	—	—
≥70	1.516	1.061–2.167	0.022
Tumor size (per cm increase)	1.074	0.996–1.159	0.065
pN status			0.004
pN0	1	—	—
pN1	1.362	0.767–2.420	0.291
pN2	1.906	1.306–2.781	0.001

CI, confidence interval; pN, pathologic nodal.

patients were 45.0%, 27.0, and 25.0%, respectively. Patients with pN0 disease showed significantly better prognosis than those with pN2 disease ($p = 0.0006$). Figure 5 shows survival curves grouped by R status; the 5-year survival rates in R0, R1, and R2 patients were 41.2%, 33.3%, and 18.4%, respectively. Patients with R0 disease showed significantly better prognosis than those with R2 disease ($p = 0.0002$). However, there were no significant differences in survival between patients with R0 and R1, and those with R1 and R2 (R0 versus R1; $p = 0.5536$; R1 versus R2; $p = 0.0915$).

The survival curves and 5-year survival rates of the T4 surgical cases grouped by age (< 70 years or ≥ 70 years) and pathologic nodal status (N0 or N1–2) are shown in Figure 6. Patients without nodal involvement and less than 70 years of age showed significantly better prognosis than those with nodal involvement and were 70 years of age or older ($p = 0.0001$; 5-year survival rate 50.3% versus 19.9%).

DISCUSSION

According to the 7th edition of the TNM staging system, the T4 stage includes invasion of the following adjacent organs: heart, mediastinal tissue, great vessels, trachea,

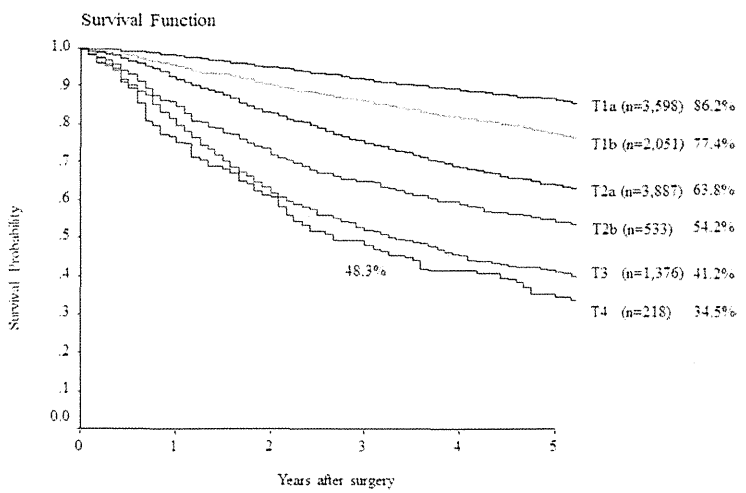

FIGURE 2. Survival curves of the 11,663 surgical cases in the Japanese Lung Cancer Registry Study grouped by pT factor International Union Against Cancer (IUCC)-Tumor Node Metastasis v. 7).

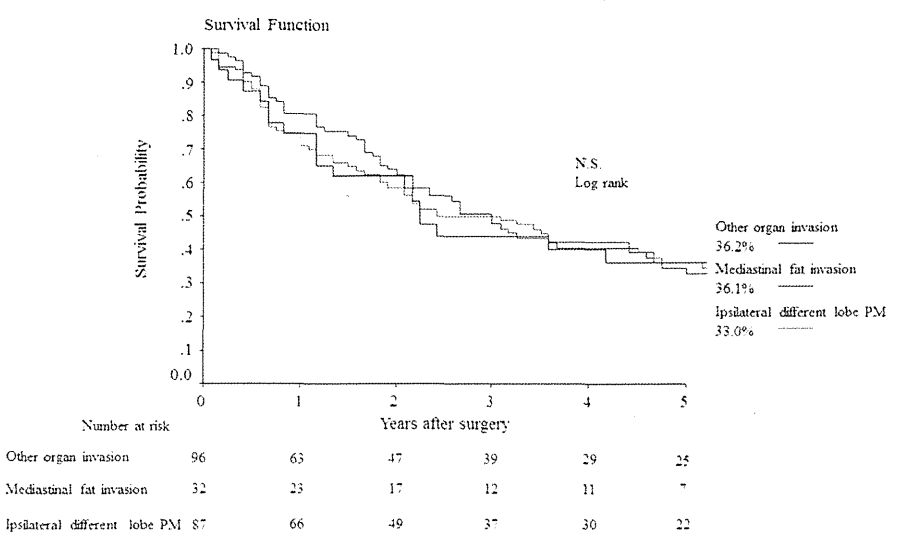

FIGURE 3. Survival curves of patients with pT4 disease grouped by reasons for being classified as T4. NS, not significant; PM, pulmonary metastasis.

TABLE 6. Types of First Recurrence by Reasons for T4 category

Reasons for T4	No. of Patients	First Recurrent Site: Local	Local + Distant	Distant	p
Mediastinal fat invasion	18	5 (28%)	4 (22%)	9 (50%)	0.487
Other organs invasion	46	8 (17%)	12 (26%)	26 (57%)	—
Ipsilateral different lobe PM	52	16 (31%)	8 (15%)	28 (54%)	—
Total	116	29 (25%)	24 (21%)	63 (54%)	—

PM, pulmonary metastasis.

recurrent laryngeal nerve, esophagus, body of vertebra, and carina.[1] Because of this great variety in neighboring organs, and the small number of resected T4 cases, there have been few review articles describing the prognosis of a substantial number of resected T4 cases.[3–6] Thus, the judgment for surgical indication is left to each institution.

Among the T4 diseases with neighboring structure invasion, mediastinal fat tissue invasion is considered to be the last step before involving other T4 organs, including mediastinal vessels, esophagus, or trachea (Fig. 1). The complete combined resection of mediastinal fat tissues adjacent to the primary tumor is technically much easier than that of other T4 organs. Therefore, we hypothesized that T4 patients with only mediastinal fat invasion might have a better prognosis than those with other T4 organ invasion or ipsilateral nonprimary lobe PM. However, the results of the present study found no significant differences in survival among these three groups with T4 disease. Although the number of patients in each T4 subset is small, these findings confirm the appropriateness of the definition of the T4 category in the current TNM staging system.

Two points constitute the prime criteria in determining the indication for resecting the neighboring organs in T4 lung cancer patients,. One is whether complete resection is possible, and the other is the length of survival that can be expected for the T4 patient even after complete resection. The presence or absence of complete resection is an absolute prognostic factor in lung cancer surgery. Although many previous reports have suggested the technical feasibility of surgery for T4 disease, fewer series have demonstrated long-term results after the extended resection.[3–6] Grunenwald et al.[7] suggested that the T4 category includes two types of disease, calling one *potentially resectable T4* and the other *definitively unresectable T4*. The potentially resectable T4 group includes cases where complete resection seems possible, based on the degree of invasion, and a better prognosis is anticipated; this group includes invasion of the carina, left atrium, superior vena cava (SVC), and mediastinal tissue. For example, in patients having tumor that directly invades the SVC, the prognosis after combined resection of the SVC is relatively good,[8–11] with a 5-year survival rate of 36%.[12] However, cases with invasion of the trachea, vertebra, and esophagus are considered to be definitively unresectable T4 because reconstruction is difficult, surgical stress is unreasonable, the operative morbidity and mortality are high, and a good prognosis cannot be expected after the resection. Grunenwald et al.[7] reported the clear identification of esophageal invasion as the worst prognostic factor,[4] and most surgeons consider invasion of the esophagus, vertebral bodies, or trachea as contraindications to surgery.

The present study was based on a nationwide registry that collected 11,663 cases during 2004 from 253 major teaching hospitals in Japan; however, only an extremely small number of surgical cases involved invasion of the esophagus, vertebra, and trachea ($n = 8$ [0.07%], $n = 6$ [0.05%], and $n = 3$

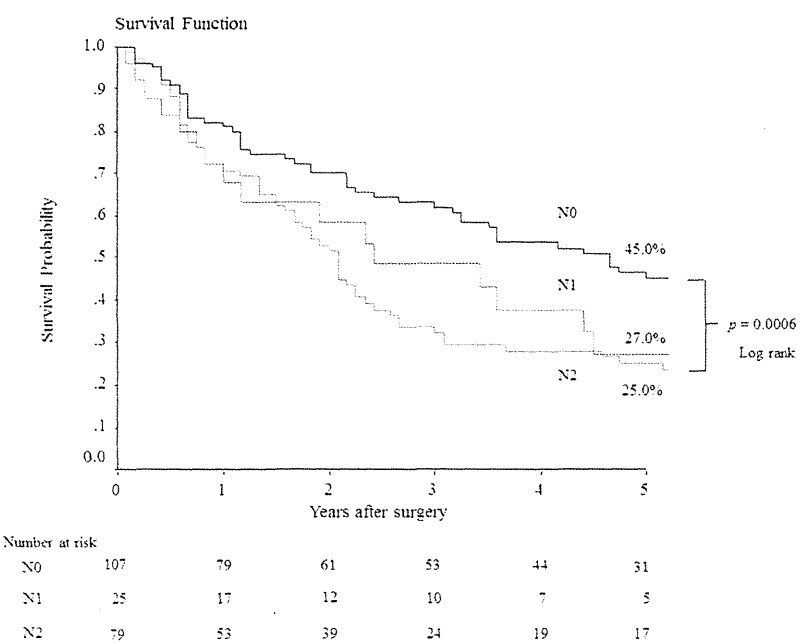

FIGURE 4. Survival curves of patients with pT4 disease grouped by pN status.

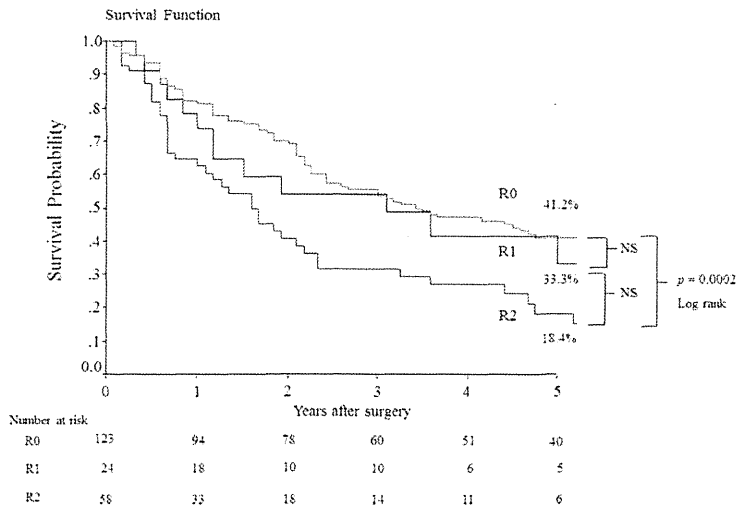

FIGURE 5. Survival curves of patients with pT4 disease grouped by R status. NS, not significant.

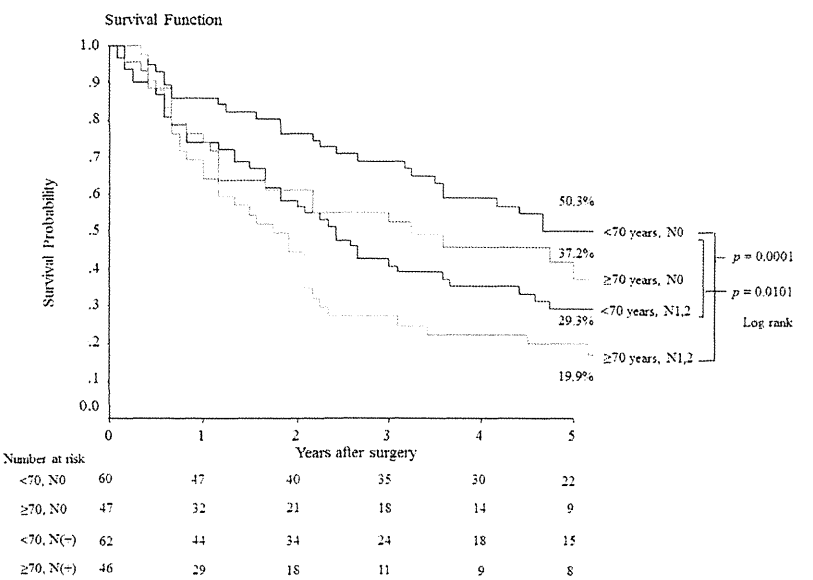

FIGURE 6. Survival curves of patients with pT4 disease grouped by age and nodal status.

[0.03%], respectively; Table 1). Overall survival of T4 surgical cases in this registration study showed better prognosis, with a 5-year survival rate of 35.4% (Fig. 2) compared with a 5-year survival rate of 22% reported in the International Association for the Study of Lung Cancer[13] staging article in 2007. These relatively good results for T4 surgical cases were probably because of the recent changes in how Japanese surgeons select T4 disease patients as surgical candidates, in accordance with the results of previous reports to determine the prognosis of resected T4 disease.[3–7] This patient selection bias may be one of the reasons why there was no significant difference in survival among the three subgroups of T4 category in our study (Fig. 3). Very low surgical mortality of these T4 patients in this registry (1 of 215; 0.47%) may support this hypothesis.

Multivariate analysis showed that nodal status was the most important prognostic factor in T4 disease (Table 5), similar to other lung cancer patients. Surgery seemed to be contraindicated in patients with mediastinal metastasis because of their poor prognosis (HR = 1.906; $p = 0.001$), as previously reported. In the TNM 7th edition, T4N0-1M0 was downstaged from stage IIIB to stage IIIA. However, the indication for N1 disease is still controversial, as some reports suggest a very poor prognosis for patients with hilar metastasis (N1). A T4N0M0 case where complete resection is possible is a good candidate for surgical treatment, as shown in Figure 4, and to perform a meticulous evaluation of the N factor through computed tomography scan, positron emission tomography scan, endobronchial ultrasound, or mediastinoscopy before any judgment is indispensable.[4–16]

In the present study, age and nodal status were revealed to be independent prognostic factors. T4 patients 70 years of age or more with any nodal involvement (N1, 2) showed poor prognosis, whereas T4 patients less than 70 years of

age without nodal involvement (N0) showed good prognosis, with a 5-year survival rate of more than 50%. There was no significant difference in the distribution of involved T4 organs between the group of patients who were 70 years of age or older and that group in which patients were less than 70 years of age, in the present study (data not shown). Because the risk–benefit ratio for extended surgical resection is very high in older T4 patients,[3] special care must be taken to decide the surgical indication, especially in node-positive T4 patients who are more than 70 years old. In particular, the outcomes after resection in patients with carinal involvement reportedly show a high average operative mortality of 17% (range, 7%–29%).[17–21] According to the evidence-based clinical practice guidelines of the American College of Chest Physicians,[17] it is recommended that surgical candidates with T4 disease should be very carefully selected, and surgical resection should be carefully undertaken only at a specialized center because of the limited survival and the high mortality. It is necessary for surgeons to collectively consider the patient's nodal status, age, quality of life after resection, the presence of alternative treatment, the extent of surgery, and subsequent morbidity and mortality before performing surgery for T4 disease.

CONCLUSION

Although T4 patients with only mediastinal fat invasion showed high incidence of R0 resection, there was no significant difference in survival between T4 patients with only mediastinal fat invasion and those with other T4 organ invasion, or ipsilateral different lobe PM, which demonstrates the appropriateness of the T4 category definition in the current TNM staging system. Patients with involvement of T4 structures should be very carefully selected for surgical resection because of the limited survival. Before undergoing surgery, patients should be subjected to careful assessment of hilar and mediastinal nodal involvement, particularly for those who are 70 years of age or older. On the basis of the findings obtained to date, the best prognosis for T4 disease is found for T4N0 patients who are less than 70 years of age and have a 5-year survival rate of more than 50%.

REFERENCES

1. Sobin LHG, Gospodarowicz MK, Wittekind C (Eds). *International Union Against Cancer (UICC) TNM Classification of Malignant Tumors*, 7th Ed. New York, NY: Wiley-Liss, 2009.
2. Sawabata N, Miyaoka E, Asamura H, et al.; Japanese Joint Committee for Lung Cancer Registration. Japanese lung cancer registry study of 11,663 surgical cases in 2004: demographic and prognosis changes over decade. *J Thorac Oncol* 2011;6:1229–1235.
3. Rice TW, Blackstone EH. Radical resections for T4 lung cancer. *Surg Clin North Am* 2002;82:573–587.
4. Grunenwald DH. Surgery for locally advanced non-small cell lung cancer. *Semin Surg Oncol* 2003;21:85–90.
5. Rusch VW, Albain KS, Crowley JJ, et al. Neoadjuvant therapy: a novel and effective treatment for stage IIIb non-small cell lung cancer. Southwest Oncology Group. *Ann Thorac Surg* 1994;58:290–4; discussion 294.
6. Pitz CC, Brutel de la Rivière A, van Swieten HA, Westermann CJ, Lammers JW, van den Bosch JM. Results of surgical treatment of T4 non-small cell lung cancer. *Eur J Cardiothorac Surg* 2003;24:1013–1018.
7. Grunenwald DH, André F, Le Péchoux C, et al. Benefit of surgery after chemoradiotherapy in stage IIIB (T4 and/or N3) non-small cell lung cancer. *J Thorac Cardiovasc Surg* 2001;122:796–802.
8. Thomas P, Magnan PE, Moulin G, Giudicelli R, Fuentes P. Extended operation for lung cancer invading the superior vena cava. *Eur J Cardiothorac Surg* 1994;8:177–182.
9. Dartevelle P, Macchiarini P, Chapelier A. Technique of superior vena cava resection and reconstruction. *Chest Surg Clin N Am* 1995;5:345–358.
10. Spaggiari L, Regnard JF, Magdeleinat P, Jauffret B, Puyo P, Levasseur P. Extended resections for bronchogenic carcinoma invading the superior vena cava system. *Ann Thorac Surg* 2000;69:233–236.
11. Spaggiari L, Magdeleinat P, Kondo H, et al. Results of superior vena cava resection for lung cancer. Analysis of prognostic factors. *Lung Cancer* 2004;44:339–346.
12. Suzuki K, Asamura H, Watanabe S, Tsuchiya R. Combined resection of superior vena cava for lung carcinoma: prognostic significance of patterns of superior vena cava invasion. *Ann Thorac Surg* 2004;78:1184–9; discussion 1184.
13. Rami-Porta R, Ball D, Crowley J, et al.; International Staging Committee; Cancer Research and Biostatistics; Observers to the Committee; Participating Institutions. The IASLC Lung Cancer Staging Project: proposals for the revision of the T descriptors in the forthcoming (seventh) edition of the TNM classification for lung cancer. *J Thorac Oncol* 2007;2:593–602.
14. Vesselle H, Pugsley JM, Vallières E, Wood DE. The impact of fluorodeoxyglucose F 18 positron-emission tomography on the surgical staging of non-small cell lung cancer. *J Thorac Cardiovasc Surg* 2002;124:511–519.
15. Gould MK, Kuschner WG, Rydzak CE, et al. Test performance of positron emission tomography and computed tomography for mediastinal staging in patients with non-small-cell lung cancer: a meta-analysis. *Ann Intern Med* 2003;139:879–892.
16. Toloza EM, Harpole L, McCrory DC. Noninvasive staging of non-small cell lung cancer: a review of the current evidence. *Chest* 2003;123:137–146S.
17. Jett JR, Schild SE, Keith RL, Kesler KA; American College of Chest Physicians. Treatment of non-small cell lung cancer, stage IIIB: ACCP evidence-based clinical practice guidelines (2nd edition). *Chest* 2007;132(3 Suppl):266S–276S.
18. Tedder M, Anstadt MP, Tedder SD, Lowe JE. Current morbidity, mortality, and survival after bronchoplastic procedures for malignancy. *Ann Thorac Surg* 1992;54:387–391.
19. Roviaro GC, Varoli F, Rebuffat C, et al. Tracheal sleeve pneumonectomy for bronchogenic carcinoma. *J Thorac Cardiovasc Surg* 1994;107:13–18.
20. Dartevelle P, Macchiarini P. Carinal resection for bronchogenic cancer. *Semin Thorac Cardiovasc Surg* 1996;8:414–425.
21. Mitchell JD. Carinal resection and reconstruction. *Chest Surg Clin N Am* 2003;13:315–329.

nature genetics

A genome-wide association study identifies two new susceptibility loci for lung adenocarcinoma in the Japanese population

Kouya Shiraishi[1], Hideo Kunitoh[2,13], Yataro Daigo[3,4], Atsushi Takahashi[5], Koichi Goto[6], Hiromi Sakamoto[7], Sumiko Ohnami[7], Yoko Shimada[1], Kyota Ashikawa[8], Akira Saito[9], Shun-ichi Watanabe[10], Koji Tsuta[11], Naoyuki Kamatani[5], Teruhiko Yoshida[7], Yusuke Nakamura[4], Jun Yokota[12], Michiaki Kubo[8] & Takashi Kohno[1]

Lung adenocarcinoma is the most common histological type of lung cancer, and its incidence is increasing worldwide. To identify genetic factors influencing risk of lung adenocarcinoma, we conducted a genome-wide association study and two validation studies in the Japanese population comprising a total of 6,029 individuals with lung adenocarcinoma (cases) and 13,535 controls. We confirmed two previously reported risk loci, 5p15.33 (rs2853677, $P_{combined} = 2.8 \times 10^{-40}$, odds ratio (OR) = 1.41) and 3q28 (rs10937405, $P_{combined} = 6.9 \times 10^{-17}$, OR = 1.25), and identified two new susceptibility loci, 17q24.3 (rs7216064, $P_{combined} = 7.4 \times 10^{-11}$, OR = 1.20) and 6p21.3 (rs3817963, $P_{combined} = 2.7 \times 10^{-10}$, OR = 1.18). These data provide further evidence supporting a role for genetic susceptibility in the development of lung adenocarcinoma.

Lung cancer is the leading cause of cancer-related death in most countries[1]. Lung cancer consists of three major histological types: adenocarcinoma, squamous-cell carcinoma and small-cell carcinoma[1–3]. Adenocarcinoma is the most common type, comprising ~40% of all cases of lung cancer, and its incidence is increasing in both Asian and Western countries. The development of lung adenocarcinoma is more weakly associated with smoking than are the developments of squamous and small-cell carcinomas, indicating that the mechanisms of carcinogenesis differ among these histological types. A better understanding of the genetic factors underlying the development of lung adenocarcinoma is strongly needed to elucidate the etiology of disease and identify high-risk individuals for targeted screening and/or prevention. In particular, the proportion of females and never smokers among patients with lung adenocarcinoma is considerably higher in Asians than in Europeans[2,3], suggesting that genetic factors contribute differently to disease in the two populations.

Genome-wide association studies (GWAS) of lung cancer with a full range of histological types have been conducted in European populations, and associations at 15q25.1, 5p15.33 and 6p21.33 have been identified[4–8]. Variants at these regions have been defined in European populations by a meta-analysis of GWAS according to histological types, and rs2736100 in *TERT* at 5p15.33 was found to be associated with risk of lung adenocarcinoma[9]. However, no additional loci reached genome-wide significance in the study; therefore, GWAS focusing on lung adenocarcinoma were greatly needed[9]. A recent GWAS on lung adenocarcinoma risk in the Japanese and Korean populations identified a new locus, 3q28 (*TP63*)[10]. Subsequently, a significant but weaker association of 3q28 variations with lung adenocarcinoma risk was validated in Europeans[11]. Notably, the association of this locus with cancer risk was supported by a recent GWAS on lung cancer with a full range of different histological types in the Chinese population[12]. These results indicate that there may be differences in the magnitude of the contribution of these loci to lung cancer susceptibility by ethnicity. Here, to further elucidate the genetic factors contributing to the development of lung adenocarcinoma, we performed a GWAS focusing on lung adenocarcinoma in the Japanese population and expanded the scale of our previous study in terms of both sample size and SNP coverage[10].

Using Illumina Omni1-Quad and OmniExpress chips, we genotyped 1,722 cases and 5,846 controls for 709,857 SNPs (**Supplementary Table 1**). Based on the results of a stringent quality-control analysis, we chose 538,166 autosomal SNPs, 1,695 cases and 5,333 control subjects for our GWAS analyses (Online Methods and

[1]Division of Genome Biology, National Cancer Center Research Institute, Tokyo, Japan. [2]Division of Thoracic Oncology, National Cancer Center Hospital, Tokyo, Japan. [3]Department of Medical Oncology, Shiga University of Medical Science, Shiga, Japan. [4]Laboratory of Molecular Medicine, Human Genome Center, Institute of Medical Science, University of Tokyo, Tokyo, Japan. [5]Laboratory for Statistical Analysis, Center for Genomic Medicine, RIKEN, Kanagawa, Japan. [6]Thoracic Oncology Division, National Cancer Center Hospital East, Chiba, Japan. [7]Division of Genetics, National Cancer Center Research Institute, Tokyo, Japan. [8]Laboratory for Genotyping Development, Center for Genomic Medicine, RIKEN, Kanagawa, Japan. [9]Statistical Genetics Analysis Division, StaGen Co. Ltd, Tokyo, Japan. [10]Division of Thoracic Surgery, National Cancer Center Hospital, Tokyo, Japan. [11]Division of Pathology and Clinical Laboratories, National Cancer Center Hospital, Tokyo, Japan. [12]Division of Multistep Carcinogenesis, National Cancer Center Research Institute, Tokyo, Japan. [13]Present address: Department of Respiratory Medicine, Mitsui Memorial Hospital, Tokyo, Japan. Correspondence should be addressed to T.K. (tkkohno@ncc.go.jp).

Received 21 February; accepted 18 June; published online 15 July 2012; doi:10.1038/ng.2353

Table 1 Summary of the GWAS and validation studies and the combined analyses

dbSNP		Allele		Cases		Controls				
locus	Gene	[risk allele]	Stage	Total	RAF	Total	RAF	P^a	OR (95% CI)	P_{het}
rs2853677	*TERT*	T/C	GWAS	1,695	0.384	5,333	0.308	8.66×10^{-17}	1.41 (1.30–1.53)	
5p15.33	intron 2	[C]	First validation	2,955	0.374	7,036	0.297	8.62×10^{-21}	1.43 (1.32–1.54)	
			Second validation	1,373	0.360	1,132	0.290	5.88×10^{-6}	1.35 (1.19–1.54)	
			Combined validation[b]	4,328	0.370	8,168	0.296	3.90×10^{-25}	1.42 (1.32–1.50)	0.49
			Combined all[b]	6,023	0.374	13,501	0.300	2.80×10^{-40}	1.41 (1.32–1.50)	0.79
rs2736100	*TERT*	T/G	GWAS	1,695	0.458	5,329	0.391	7.31×10^{-12}	1.32 (1.22–1.42)	
5p15.33	intron 2	[G]	First validation	2,954	0.458	7,036	0.385	2.13×10^{-19}	1.39 (1.29–1.49)	
			Second validation	1,343	0.432	1,166	0.368	1.79×10^{-4}	1.27 (1.12–1.44)	
			Combined validation[b]	4,297	0.450	8,202	0.383	3.97×10^{-22}	1.36 (1.28–1.44)	0.22
			Combined all[b]	5,992	0.452	13,531	0.386	2.50×10^{-32}	1.34 (1.28–1.41)	0.39
rs10937405	*TP63*	C/T	GWAS	1,695	0.728	5,333	0.677	1.10×10^{-8}	1.29 (1.18–1.40)	
3q28	intron 1	[C]	First validation	2,953	0.714	7,036	0.663	9.22×10^{-10}	1.27 (1.18–1.37)	
			Second validation	1,375	0.704	1,166	0.682	1.22×10^{-1}	1.11 (0.97–1.26)	
			Combined validation[b]	4,328	0.711	8,202	0.666	8.17×10^{-10}	1.23 (1.15–1.31)	0.076
			Combined all[b]	6,023	0.715	13,535	0.670	6.92×10^{-17}	1.25 (1.19–1.32)	0.15
rs7216064	*BPTF*	A/G	GWAS	1,695	0.747	5,333	0.706	1.07×10^{-5}	1.22 (1.12–1.34)	
17q24.3	intron 9	[A]	First validation	2,955	0.736	7,036	0.708	7.72×10^{-5}	1.17 (1.08–1.27)	
			Second validation	1,376	0.744	1,166	0.708	4.70×10^{-3}	1.21 (1.06–1.39)	
			Combined validation[b]	4,331	0.739	8,202	0.708	1.34×10^{-6}	1.18 (1.10–1.26)	0.65
			Combined all[b]	6,026	0.741	13,535	0.707	7.40×10^{-11}	1.20 (1.13–1.26)	0.76
rs3817963	*BTNL2*	A/G	GWAS	1,695	0.363	5,331	0.327	5.54×10^{-5}	1.18 (1.09–1.28)	
6p21.3	intron 4	[G]	First validation	2,951	0.347	7,028	0.310	1.59×10^{-5}	1.18 (1.09–1.27)	
			Second validation	1,376	0.358	1,166	0.329	2.41×10^{-2}	1.16 (1.02–1.32)	
			Combined validation[b]	4,327	0.350	8,194	0.313	1.14×10^{-6}	1.17 (1.10–1.25)	0.86
			Combined all[b]	6,022	0.354	13,525	0.318	2.69×10^{-10}	1.18 (1.12–1.24)	0.97

RAF, risk allele frequency; P_{het}, *P* value for heterogeneity.
[a]Adjusted for age and gender. [b]The combined meta-analysis was performed using a fixed effect model.

Supplementary Fig. 1). We generated a quantile-quantile plot using the results of a logistic regression trend test (**Supplementary Fig. 1d**). The genomic inflation factor ($\lambda_{1,000}$)[13] was 1.021, indicating a low possibility of false-positive associations resulting from population stratification or genotype misclassification (**Supplementary Fig. 2**).

In the GWAS, two loci reached genome-wide significance for association ($P < 5 \times 10^{-8}$; **Supplementary Fig. 1e**); these two loci have been reported in previous GWAS (rs2736100 at 5p13.33 and rs10937405 at 3q28)[9,10]. We also identified a significant association for a SNP (rs2853677 at 5p13.33) that was not examined in our previous GWAS (**Table 1**). In addition, we examined associations of other previously reported loci with lung cancer risk (**Supplementary Table 2**). We found one locus (rs2131877 at 3q29)[14] to be associated with lung adenocarcinoma risk, but we could not confirm the associations between lung adenocarcinoma risk and the other loci identified in a recent GWAS of the European and Han Chinese populations[12]. These results are probably the result of the lower statistical power in our GWAS than in the previous GWAS (**Supplementary Table 2**). In addition, most of the earlier GWAS were performed in lung cancer representing a full range of histological types and in subjects of European descent. Therefore, differences in genetic modifiers and/or environmental factors in different histological types and populations might have contributed to the differing results.

To investigate additional susceptibility loci, we conducted a validation study using two independent sample sets consisting of 2,955 cases and 7,036 controls (first validation cohort) and 1,379 cases and 1,166 controls (second validation cohort) (**Supplementary Table 1**). Among 125 SNPs with a logistic regression trend of $P < 1 \times 10^{-4}$ in our GWAS, we selected 78 SNPs, excluding 38 SNPs within the same locus ($r^2 > 0.8$) and nine SNPs located at the previously reported loci, 5p13.33 and 3q28. We successfully genotyped all 78 SNPs in the first validation set using the multiplex PCR-based Invader assay, and 8 SNPs had ORs with a significance of $P < 0.05$ in the same direction of association (**Supplementary Table 3**). We then subjected these eight SNPs to the second validation set analysis. When we combined the results of both validation sets using a fixed effects model, two SNPs, rs7216064 at 17q24.3 and rs3817963 at 6p21.3, showed significant associations after Bonferroni correction ($P < 6.4 \times 10^{-4}$, calculated as 0.05/78) in addition to three SNPs at the two known loci described above (**Table 1**). When we combined the results of the GWAS and the validation study, both of the newly discovered loci reached genome-wide significance (rs7216064, $P = 7.4 \times 10^{-11}$, OR = 1.20; rs3817963, $P = 2.7 \times 10^{-10}$, OR = 1.18) (**Table 1**). The ORs were similar between the GWAS and the validation study, with no heterogeneity (**Table 1**). The strengths of the associations remained similar after adjustment for smoking (**Supplementary Table 4**). In a subgroup analysis (**Supplementary Table 5**), there was no clear association between the two newly discovered loci and gender or smoking behavior, and there was also no such association for the two known loci[10].

We next performed imputation analyses using the Japanese in Tokyo (JPT) and Han Chinese in Beijing (CHB) reference sets from the 1000 Genomes Project database (June 2010 release) (Online Methods), and we examined the associations between 1,665 putative SNPs and lung adenocarcinoma risk. We found a series of signals in high linkage disequilibrium (LD) with a marker SNP at 17q24.3 (rs7216064), and we observed significant associations with lung adenocarcinoma risk for 33 of the imputed SNPs (**Fig. 1a** and **Supplementary Table 6**). However, none of the SNPs in LD at 6p21.3 reached the *P* value of our marker SNP (**Fig. 1b**).

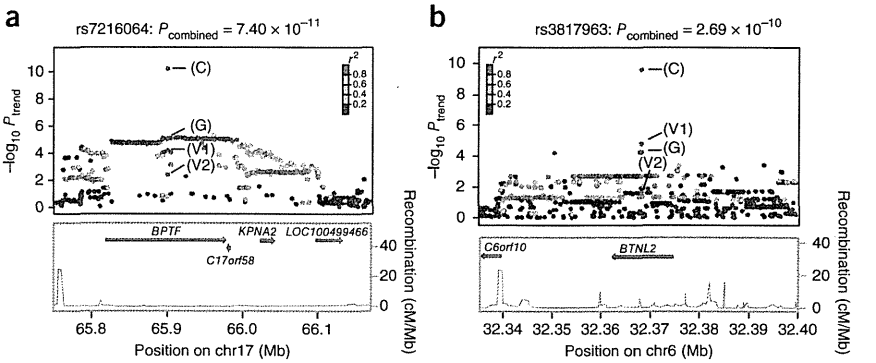

Figure 1 Regional plots of the identified marker SNPs. (**a**) rs7216064 at 17q24.3. (**b**) rs3817963 at 6p21.3. The marker SNP is shown in purple, and the r^2 values for the other SNPs are indicated by different colors. The correlations were estimated using data from the 1000 Genomes Project. The genes within the region of interest are annotated and are indicated by arrows. The blue lines indicate the recombination rates in cM per Mb. The $-\log_{10} P_{trend}$ values of the marker SNPs are shown for the GWAS (G), the first validation study (V1), the second validation study (V2) and the combined study (C).

SNP rs7216064 resides within intron 9 of *BPTF* (encoding bromodomain PHD finger transcription factor) at 17q24.3. Other imputed SNPs in this locus showing similarly significant associations were also synonymous (not resulting in amino acid changes in translated proteins). Based on the regional plot and recombination rates, we found that rs7216064 represented an LD region that includes three genes: *BPTF*, *C17orf58* (encoding a protein without known domains) and *KPNA2* (encoding karyopherin α 2) (**Fig. 1a**). Thus, to address the biological importance of 17q24.3 variants, we examined the mRNA expression levels of these three genes in 314 noncancerous lung tissues by real-time quantitative PCR (**Supplementary Note**). We detected expression of *BPTF*, but not of *C17orf58* or *KPNA2*, in these lung tissues. The expression of *BPTF* was marginally different depending on the genotype of the rs7216064 SNP ($P = 0.02$), implying low expression from the risk (G) allele (**Supplementary Table 7**). *BPTF* encodes a chromatin remodeling factor that regulates transcription through the specific recognition of methylated histone proteins[15]. Recently, chromatin remodeling genes have been implicated as tumor suppressors in lung[16] and other cancers[17]. Therefore, a low level of *BPTF* mRNA being associated with the risk allele might lead to an elevated risk for lung adenocarcinoma through decreased transcriptional regulation. However, further studies are needed to conclude whether *BPTF* is responsible for lung adenocarcinoma susceptibility.

SNP rs3817963 is located in intron 4 of *BTNL2* (encoding butyrophilin-like 2) at 6p21.3 (**Fig. 1b**). Based on the regional plot and recombination rates, rs3817963 represents an LD region that includes only a single gene, *BTNL2*. The top ten SNPs (genotyped or imputed), including rs3817963, were synonymous. The effects of the SNPs on the expression of *BTNL2* could not be assessed because of the low or absent expression of this gene in noncancerous lung tissues. *BTNL2* encodes a T cell co-stimulatory molecule, and associations between *BTNL2* SNPs and risk have been reported in several immune-related diseases, including asthma[18], vitiligo[19] and ulcerative colitis[20,21]. Therefore, *BTNL2* might affect lung adenocarcinoma risk by affecting immune responses against tumor cells. However, 6p21.3 is a part of the extended major histocompatibility complex (MHC) region, whose association with lung cancer risk has previously been reported[5]. The previously identified marker SNPs, rs3117582 and rs3131379, located 700 kb from the *BTNL2* locus, were monomorphic in our study populations. Therefore, it is possible that the association at 6p21.3 identified in the present study is not new, and further studies are warranted.

We here provide further evidence for the existence of genetic susceptibility in the development of lung adenocarcinoma through the identification of two candidate susceptibility loci, 17q24.3 and 6p21.3, at genome-wide significance. rs7216064 at 17q24.3 showed a tendency of association in the same direction as lung cancer risk in Europeans, although this association did not reach statistical significance, whereas rs3135353 at 6p21.3, which is in LD with rs3817963, showed a statistically significant association with lung cancer risk in European and American populations (**Supplementary Table 8**)[7,9]. Therefore, these loci might be involved in lung cancer risk in individuals of European descent. Further studies of these loci in multiple populations, including those with other histological types of lung cancers, will help to elucidate the etiology of lung adenocarcinoma.

URLs. The BioBank Japan project, http://biobankjp.org/; R, http://cran.r-project.org/; PLINK statistical software v1.06, http://pngu.mgh.harvard.edu/~purcell/plink/; Primer3 v0.3.0, http://frodo.wi.mit.edu/primer3/; UCSC Genome Browser, http://genome.ucsc.edu/; LocusZoom, http://csg.sph.umich.edu/locuszoom/; a catalog of genome-wide association studies, http://www.genome.gov/gwastudies/; SNPinfo Web Server, http://manticore.niehs.nih.gov/index.html; Illumina's IconDB resource, http://www.illumina.com/science/icontroldb.ilmn.

METHODS

Methods and any associated references are available in the online version of the paper.

Note: Supplementary information is available in the online version of the paper.

ACKNOWLEDGMENTS

We thank all of the subjects for participating in the study, and we also thank the collaborating physicians for assisting with sample collection. We are grateful to the members of BioBank Japan, the National Cancer Center Biobank and the Rotary Club of Osaka-Midosuji District 2660 Rotary International in Japan for supporting our study. We thank Y. Aoi, T. Odaka, M. Okuyama, H. Totsuka, S. Chiku, A. Kuchiba and the technical staff of the Center for Genome Medicine, National Cancer Center Research Institute, for providing technical and methodological assistance. We also thank H. Hirose of Health Center, Keio University and D. Saito of National Cancer Center Hospital (present affiliation: Nihonbashi Daizo Clinic) for DNA samples of control subjects. This work was supported in part by Grants-in-Aid from the Ministry of Health, Labor and Welfare for Research on Applying Health Technology and for the 3rd-term Comprehensive 10-year Strategy for Cancer Control; from the Ministry of Education, Culture, Sports, Science and Technology of Japan for Scientific Research on Innovative Areas (22131006); from the Japan Society for the Promotion of Science for Research Activity Start-up (23800073) and for Young Scientists (B) (24790340); and by the National Cancer Center Research and Development Fund. This work was also conducted as a part of the BioBank Japan Project supported by the Ministry of Education, Culture, Sports, Science and Technology, Japan. The National Cancer Center Biobank is supported by the National Cancer Center Research and Development Fund, Japan.

AUTHOR CONTRIBUTIONS

K.S., J.Y., M.K. and T.K. designed the study. A.T., K.A., S.O., N.K. and A.S. analyzed the GWAS and replication study. H.S., Y.S., T.Y. and K.S. performed the genotyping for the GWAS and the replication study. H.K., K.G., S.W. and K.T. recruited

subjects and participated in diagnostic evaluations. K.S. and T.K. wrote the manuscript. M.K., Y.D., T.Y. and Y.N. contributed to the overall GWAS design.

COMPETING FINANCIAL INTERESTS

The authors declare no competing financial interests.

Published online at http://www.nature.com/doifinder/10.1038/ng.2353.
Reprints and permissions information is available online at http://www.nature.com/reprints/index.html.

1. Colvy, T.V. *et al.* Adenocarcinoma. in *World Health Organization Classification of Tumors: Pathology and Genetics, Tumours of Lung, Pleura, Thymus and Heart* (eds. Travis, W.D., Brambilla, E., Muller-Hermelink, H.K. & Harris, C.C.) 35–44 (IARC Press, Lyon, France, 2004).
2. Subramanian, J. & Govindan, R. Lung cancer in never smokers: a review. *J. Clin. Oncol.* **25**, 561–570 (2007).
3. Sun, S., Schiller, J.H. & Gazdar, A.F. Lung cancer in never smokers—a different disease. *Nat. Rev. Cancer* **7**, 778–790 (2007).
4. Broderick, P. *et al.* Deciphering the impact of common genetic variation on lung cancer risk: a genome-wide association study. *Cancer Res.* **69**, 6633–6641 (2009).
5. Wang, Y. *et al.* Common 5p15.33 and 6p21.33 variants influence lung cancer risk. *Nat. Genet.* **40**, 1407–1409 (2008).
6. McKay, J.D. *et al.* Lung cancer susceptibility locus at 5p15.33. *Nat. Genet.* **40**, 1404–1406 (2008).
7. Hung, R.J. *et al.* A susceptibility locus for lung cancer maps to nicotinic acetylcholine receptor subunit genes on 15q25. *Nature* **452**, 633–637 (2008).
8. Amos, C.I. *et al.* Genome-wide association scan of tag SNPs identifies a susceptibility locus for lung cancer at 15q25.1. *Nat. Genet.* **40**, 616–622 (2008).
9. Landi, M.T. *et al.* A genome-wide association study of lung cancer identifies a region of chromosome 5p15 associated with risk for adenocarcinoma. *Am. J. Hum. Genet.* **85**, 679–691 (2009).
10. Miki, D. *et al.* Variation in *TP63* is associated with lung adenocarcinoma susceptibility in Japanese and Korean populations. *Nat. Genet.* **42**, 893–896 (2010).
11. Wang, Y. *et al.* Variation in *TP63* is associated with lung adenocarcinoma in the UK population. *Cancer Epidemiol. Biomarkers Prev.* **20**, 1453–1462 (2011).
12. Hu, Z. *et al.* A genome-wide association study identifies two new lung cancer susceptibility loci at 13q12.12 and 22q12.2 in Han Chinese. *Nat. Genet.* **43**, 792–796 (2011).
13. Freedman, M.L. *et al.* Assessing the impact of population stratification on genetic association studies. *Nat. Genet.* **36**, 388–393 (2004).
14. Yoon, K.A. *et al.* A genome-wide association study reveals susceptibility variants for non-small cell lung cancer in the Korean population. *Hum. Mol. Genet.* **19**, 4948–4954 (2010).
15. Ruthenburg, A.J. *et al.* Recognition of a mononucleosomal histone modification pattern by BPTF via multivalent interactions. *Cell* **145**, 692–706 (2011).
16. Medina, P.P. & Sanchez-Cespedes, M. Involvement of the chromatin-remodeling factor BRG1/SMARCA4 in human cancer. *Epigenetics* **3**, 64–68 (2008).
17. Wilson, B.G. & Roberts, C.W. SWI/SNF nucleosome remodellers and cancer. *Nat. Rev. Cancer* **11**, 481–492 (2011).
18. Hirota, T. *et al.* Genome-wide association study identifies three new susceptibility loci for adult asthma in the Japanese population. *Nat. Genet.* **43**, 893–896 (2011).
19. Jin, Y. *et al.* Variant of *TYR* and autoimmunity susceptibility loci in generalized vitiligo. *N. Engl. J. Med.* **362**, 1686–1697 (2010).
20. Asano, K. *et al.* A genome-wide association study identifies three new susceptibility loci for ulcerative colitis in the Japanese population. *Nat. Genet.* **41**, 1325–1329 (2009).
21. Anderson, C.A. *et al.* Meta-analysis identifies 29 additional ulcerative colitis risk loci, increasing the number of confirmed associations to 47. *Nat. Genet.* **43**, 246–252 (2011).

ONLINE METHODS

Study design and subjects. We performed a three-stage GWAS of lung adenocarcinoma in the Japanese population using independent samples. The characteristics of each case-control group are shown in **Supplementary Table 1**. The discovery GWAS samples consisted of 1,722 cases from the National Cancer Center Hospital (NCCH) and 5,846 controls from the BioBank Japan project[22], Osaka-Midosuji Rotary Club (MRC) and the Pharma SNP consortium (PSC). The BioBank Japan project (see URLs) was begun in 2003 for the collection of genomic DNA, serum and clinical information from 300,000 individuals diagnosed with any of 47 diseases by a collaboration network of 66 hospitals in all areas of Japan[22]. The subjects from MRC were 1,018 healthy volunteers, and the subjects from PSC were 906 Japanese healthy volunteers from whom immortalized B lymphoblast cell lines were established by the PSC. The cell lines were obtained from the Japan Health Sciences Foundation (JHSF)/Health Science Research Resources Bank (HSRRB). Individuals with any cancer were excluded from the control group.

The validation study consisted of two independent cohorts. The first validation cohort included 2,955 cases with lung adenocarcinoma and 7,036 controls. The cases included 1,747 subjects from the BioBank Japan project and 1,208 subjects from NCCH. All control subjects were from the BioBank Japan project. Individuals with any cancer were excluded from the control group. The second validation cohort included 1,379 cases with lung adenocarcinoma from the NCCH and 1,166 controls (cancer-free volunteers) from the NCCH and the Keio University in Tokyo[23]. Individuals with any cancer were excluded from the control group.

All of the cases with lung adenocarcinoma were diagnosed by cytological and/or histological examination according to the World Health Organization classification[24]. The cases from NCCH in the GWAS and first validation sets consisted of cases for which enough DNA for large-scale SNP analyses were available, and the cases in thee second validation set consisted of cases for which less DNA were available, for example, because only small noncancerous tissues were available for DNA extraction. Controls from the BioBank Japan project were genotyped previously. Genome-wide genotyping data obtained before and after 2010 were used as the controls for the GWAS and the first validation study described below, respectively, and thus there was no specified rationale for the selection of control subjects other than time of genotyping. Eight controls and 1,529 cases with lung adenocarcinoma from BioBank Japan and 906 control subjects from the Osaka-MRC were used in the previous GWAS[10]. All the participants provided written informed consent. This project was approved by the ethical committees of each participating institution.

Sample preparation and genotyping. Genomic DNA was extracted from peripheral blood leukocytes or noncancerous lung tissues using standard methods.

In the GWAS, we genotyped 1,722 cases with lung adenocarcinoma from the NCCH using the Illumina HumanOmni1-Quad Chip. For the controls in the GWAS, we used genome-wide data from 5,846 individuals with cerebral aneurysms, chronic obstructive pulmonary disease or glaucoma, which were genotyped using the Illumina Human OmniExpress Genotyping BeadChip.

In the study of the first validation cohort, we genotyped 2,955 cases with lung adenocarcinoma using the multiplex PCR-based Invader assay (Third Wave Technologies), as previously described[10]. The control group consisted of genome-wide data from 7,036 individuals with epilepsy, nephrosis syndrome, atopic dermatitis, urinary tract stone disease or Basedow's (Graves') disease, which were genotyped using the Illumina Human OmniExpress Genotyping BeadChip. The same quality control criteria were applied as in the GWAS (see below) to confirm that no unexpected duplicates or probable relatives were present between the control subjects of the GWAS and those of the first validation study.

In the study of the second validation cohort, we genotyped 1,379 cases with lung adenocarcinoma and 1,166 controls using the TaqMan method, according to the protocol for the ABI PRISM 7900HT Sequence Detection System (Applied Biosystems).

Quality control. Systemic quality control was performed on the raw genotyping data from 709,857 SNPs in DNA samples obtained from 7,568 subjects, consisting of 1,722 cases and 5,846 controls, using PLINK (v 1.06)[25]. Forty-four subjects were excluded because they showed gender discrepancies based on their X chromosome genotypes (7,524 subjects remained). Next, SNPs were excluded according to the following criteria: (i) 19,993 SNPs were not mapped on autosomal chromosomes; (ii) 102,929 SNPs had a minor allele frequency <0.01; and (iii) a total of 48,769 SNPs had a call rate <0.99 and genotype distributions that clearly deviated from those expected by Hardy-Weinberg equilibrium ($P < 1.0 \times 10^{-6}$). Together, 538,166 SNPs in autosomal chromosomes passed the quality-control filters and were used for the GWAS.

Next, an additional 75 unexpected duplicates or probable relatives in the GWAS were excluded based on pairwise identity by state according to their PI_HAT values in PLINK (all PI_HAT > 0.25) (7,449 subjects remained). Heterozygosity rates were calculated using PLINK, and more than 6 s.d. from the mean was used as the exclusion criterion. A principal components analysis (PCA) was performed on the genotype data from the samples, along with European (CEU), African (YRI) and east Asian (Japanese (JPT)) and Han Chinese (CHB)) individuals obtained from the phase II HapMap database using smartpca[26]. The PCA revealed no evident population substructure (**Supplementary Fig. 1a**) and identified seven outliers for exclusion (7,442 subjects remained). Most subjects fell into a known main cluster (Hondo) of the Japanese population (**Supplementary Fig. 1b**), and 414 subjects that fell far from the Hondo cluster[27] were excluded. The remaining 7,028 subjects, consisting of 1,695 cases and 5,333 control subjects, were used for the GWAS. The lack of population substructure between the cases and controls was validated by PCA of the subjects in the Hondo cluster (**Supplementary Fig. 1c**).

Statistical analyses. In the GWAS and the validation study, the statistical significance of the association with each SNP was assessed using a logistic regression trend test in the R program. Age and gender were included as covariates. Heterogeneity across the two stages was examined using the Breslow-Day test[28].

Imputation. We performed SNP imputation for each individual in the GWAS using the IMPUTE7 program[29]. The 1000 Genomes Project database (June 2010 release) was used as a reference panel. After excluding imputed SNPs with a low genotype information content (<0.5), posterior probability score (<0.90), call rate (<0.90), minor allele frequency (<0.01) or Hardy-Weinberg equilibrium ($P < 1.0 \times 10^{-7}$), imputed SNPs with $r^2 > 0.3$, residing 200–500 kb upstream or downstream of the two newly identified marker SNPs, were subjected to association analyses.

Software. For general statistical analyses, we used the R statistical environment version 2.6.1 or PLINK1.06 (ref. 25). We used LocusZoom to plot regional association plots[30].

22. Nakamura, Y. The BioBank Japan Project. *Clin. Adv. Hematol. Oncol.* **5**, 696–697 (2007).
23. Kohno, T. *et al.* Individuals susceptible to lung adenocarcinoma defined by combined *HLA-DQA1* and *TERT* genotypes. *Carcinogenesis* **31**, 834–841 (2010).
24. Travis, W.D. *et al. World Health Organization. International Histological Classification of Tumors: Histological Typing of Lung and Pleural Tumors* (eds. Travis, W.D., Colby, T.V., Corrin, B., Shimosato, Y. & Brambilla, E.) (Springer-Verlag, Heidelberg, Germany, 1999).
25. Purcell, S. *et al.* PLINK: a tool set for whole-genome association and population-based linkage analyses. *Am. J. Hum. Genet.* **81**, 559–575 (2007).
26. Price, A.L. *et al.* Principal components analysis corrects for stratification in genome-wide association studies. *Nat. Genet.* **38**, 904–909 (2006).
27. Yamaguchi-Kabata, Y. *et al.* Japanese population structure, based on SNP genotypes from 7003 individuals compared to other ethnic groups: effects on population-based association studies. *Am. J. Hum. Genet.* **83**, 445–456 (2008).
28. Breslow, N.E. & Day, N.E. *Statistical Methods in Cancer Research. Volume II—The Design and Analysis of Cohort Studies* 2–333 (IARC Scientific Publications, Lyon, France, 1987).
29. Marchini, J., Howie, B., Myers, S., McVean, G. & Donnelly, P. A new multipoint method for genome-wide association studies by imputation of genotypes. *Nat. Genet.* **39**, 906–913 (2007).
30. Pruim, R.J. *et al.* LocusZoom: regional visualization of genome-wide association scan results. *Bioinformatics* **26**, 2336–2337 (2010).

doi:10.1038/ng.2353

nature medicine

KIF5B-RET fusions in lung adenocarcinoma

Takashi Kohno[1,15], Hitoshi Ichikawa[2,15], Yasushi Totoki[3], Kazuki Yasuda[4], Masaki Hiramoto[4], Takao Nammo[4], Hiromi Sakamoto[2], Koji Tsuta[5], Koh Furuta[5], Yoko Shimada[1], Reika Iwakawa[6], Hideaki Ogiwara[1], Takahiro Oike[6], Masato Enari[7], Aaron J Schetter[8], Hirokazu Okayama[6,8], Aage Haugen[9], Vidar Skaug[9], Suenori Chiku[10], Itaru Yamanaka[11], Yasuhito Arai[3], Shun-ichi Watanabe[12], Ikuo Sekine[13], Seishi Ogawa[14], Curtis C Harris[8], Hitoshi Tsuda[5], Teruhiko Yoshida[2], Jun Yokota[6] & Tatsuhiro Shibata[3]

We identified in-frame fusion transcripts of *KIF5B* (the kinesin family 5B gene) and the *RET* oncogene, which are present in 1–2% of lung adenocarcinomas (LADCs) from people from Japan and the United States, using whole-transcriptome sequencing. The *KIF5B-RET* fusion leads to aberrant activation of RET kinase and is considered to be a new driver mutation of LADC because it segregates from mutations or fusions in *EGFR*, *KRAS*, *HER2* and *ALK*, and a RET tyrosine kinase inhibitor, vandetanib, suppresses the fusion-induced anchorage-independent growth activity of NIH3T3 cells.

A considerable proportion of LADCs, the most common histological type of lung cancer that comprises ~40% of the total cases, develops through activation of oncogenes, for example, somatic mutations in *EGFR* (10–50% of cases) or *KRAS* (10–30% of cases) or fusion of *ALK* (5% of cases), in a mutually exclusive manner[1–4]. Tyrosine kinase inhibitors (TKIs) targeting the EGFR and ALK proteins are effective in the treatment of LADCs that carry *EGFR* mutations and *ALK* fusions[1–3], respectively.

We performed whole-transcriptome sequencing (RNA sequencing)[5] of 30 LADC specimens from Japanese individuals to identify new chimeric fusion transcripts that could be targets for therapy[3,5,6]. These LADCs were 2 carcinomas with *EML4-ALK* fusions, 4 with *EGFR* or *KRAS* mutations and 24 without these fusions or mutations (**Supplementary Table 1**). Identifying candidate fusions represented by >20 paired-end reads and validation by Sanger sequencing of the RT-PCR products (**Supplementary Methods**) led to the identification of seven fusion transcripts, including *EML4-ALK* (**Supplementary Table 1**). We detected one of these fusions between *KIF5B* on chromosome 10p11.2 and *RET* on chromosome 10q11.2 in subject BR0020 (**Fig. 1** and **Supplementary Fig. 1a**). We then further investigated this fusion, as fusions between *RET* and genes other than *KIF5B* have previously been shown to drive papillary thyroid tumor formation[6,7].

RT-PCR and a Sanger sequencing analysis of 319 LADC specimens from Japanese individuals (**Supplementary Table 2**), including 30 that had been subjected to whole-transcriptome sequencing, revealed that 1.9% (6 out of 319) expressed *KIF5B-RET* fusion transcripts (**Fig. 1b** and **Supplementary Fig. 1b**). We identified four variants in these six tumors, and all of these variants were in frame (**Fig. 1a**).

A genomic PCR analysis of the six tumors that were positive for RET fusions revealed somatic fusions of the *KIF5B* introns 15, 16, 23 or 24 at chromosome 10p11.2 with the *RET* introns 7 or 11 at 10q11.2 (**Supplementary Fig. 1c,d**), indicating that a chromosomal inversion had occurred between the long and short arms in the centromeric region of chromosome 10 (**Supplementary Figs. 1e** and **2**). We verified this chromosomal inversion using fluorescence *in situ* hybridization, which revealed a split in the signals for the probes that flank the *RET* translocation sites in tumors positive for the *KIF5B-RET* fusion (**Supplementary Fig. 2**).

The tumors positive for the *KIF5B-RET* fusion were all well or moderately differentiated (**Table 1** and **Supplementary Fig. 3**). None of the subjects with these tumors had a history of thyroid cancer, and none showed abnormal findings in their thyroid tissues as determined by computed tomography or positron emission tomography before surgery for LADC. All five examined tumors with the *KIF5B-RET* fusion were positive for thyroid transcription factor 1 (TTF-1) and napsin A aspartic proteinase (Napsin A)[8] but were negative for thyroglobulin[9], indicating that they were of pulmonary origin (**Table 1** and **Supplementary Fig. 3**). The LADCs that were positive for the *KIF5B-RET* fusion showed twofold to 30-fold higher *RET* expression than non-cancerous lung tissues (**Fig. 1b** and **Supplementary Figs. 4** and **5**). An immunohistochemical analysis using an antibody against the C-terminal region of the RET protein detected positive cytoplasmic staining in the tumor cells of the fusion-positive LADCs (**Table 1** and **Supplementary Fig. 3b**) but did not detect this staining in any of the non-cancerous lung cells. A western blot analysis confirmed the expression of the fusion proteins in the LADCs (**Supplementary Fig. 6**).

To address the prevalence of *KIF5B-RET* fusions in LADCs from individuals of non-Asian ancestry, we examined LADCs in cohorts from the United States and Norway (**Supplementary Table 2**). We detected a fusion transcript in 1 of the 80 (1.3%) subjects from the

[1]Division of Genome Biology, National Cancer Center Research Institute, Chuo-ku, Tokyo, Japan. [2]Division of Genetics, National Cancer Center Research Institute, Chuo-ku, Tokyo, Japan. [3]Division of Cancer Genomics, National Cancer Center Research Institute, Chuo-ku, Tokyo, Japan. [4]Department of Metabolic Disorder, Diabetes Research Center, Research Institute, National Center for Global Health and Medicine, Shinjuku-ku, Tokyo, Japan. [5]Division of Pathology and Clinical Laboratories, National Cancer Center Hospital, Chuo-ku, Tokyo, Japan. [6]Division of Multistep Carcinogenesis, National Cancer Center Research Institute, Chuo-ku, Tokyo, Japan. [7]Division of Refractory Cancer Research, National Cancer Center Research Institute, Chuo-ku, Tokyo, Japan. [8]Laboratory of Human Carcinogenesis, Center for Cancer Research, National Cancer Institute, US National Institutes of Health, Bethesda, Maryland, USA. [9]Section of Toxicology, Department of Chemical and Biological Working Environment, National Institute of Occupational Health, Oslo, Norway. [10]Science Solutions Division, Mizuho Information and Research Institute, Chiyoda-ku, Tokyo, Japan. [11]Statistical Genetics Analysis Division, StaGen, Taito-ku, Tokyo, Japan. [12]Division of Thoracic Surgery, National Cancer Center Hospital, Chuo-ku, Tokyo, Japan. [13]Division of Thoracic Oncology, National Cancer Center Hospital, Chuo-ku, Tokyo, Japan. [14]Cancer Genomics Project, University of Tokyo, Bunkyo-ku, Tokyo, Japan. [15]These authors equally contributed to this work. Correspondence should be addressed to T.K. (tkkohno@ncc.go.jp).

Received 23 August 2011; accepted 16 December 2011; published online 12 February 2012; doi:10.1038/nm.2644

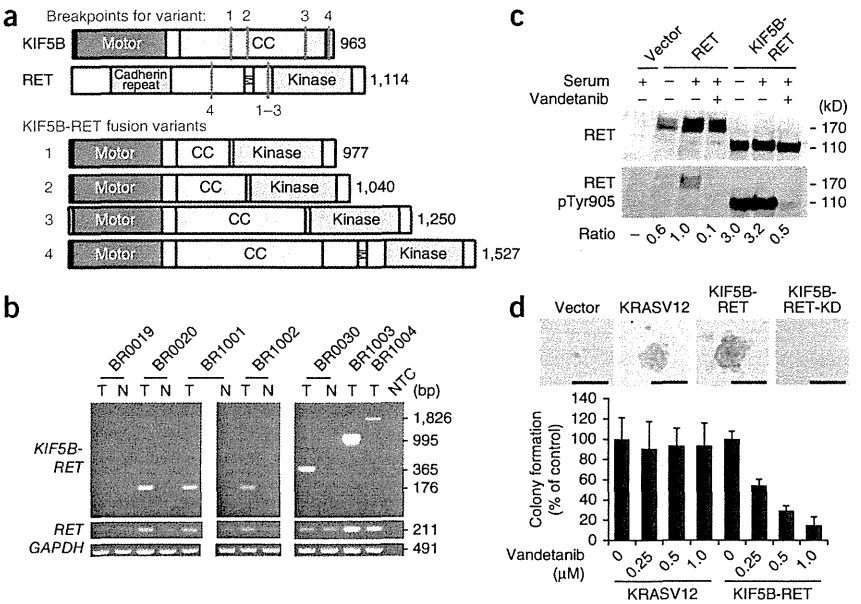

Figure 1 *KIF5B-RET* fusions in LADC. (**a**) Schematic representations of the wild-type KIF5B and RET proteins as well as the four fusion variants identified in this study. The breakpoints for each variant are indicated with red lines. CC, coiled coil; TM, transmembrane. (**b**) Detection of *KIF5B-RET* fusions by RT-PCR. RT-PCR products for the *RET* kinase domain (exons 12 and 13) and *GAPDH* are shown below. Six LADCs positive for *KIF5B-RET* fusions (T) are shown, with four corresponding non-cancerous lung tissues (N), a no-template control (NTC) and one LADC that was negative for the fusion (BR0019). (**c**) Activation of RET kinase activity in the KIF5B-RET protein and the suppression of this activity by vandetanib. H1299 lung cancer cells were transfected with an empty vector, wild-type RET (RET) or KIF5B-RET expression plasmids and treated either with DMSO (serum) or vandetanib, as indicated. The ratios of phosphorylated Tyr905 (pTyr905) RET to total RET signals with respect to wild-type RET after the serum treatment are listed below the gels. (**d**) Anchorage-independent growth of NIH3T3 cells expressing KIF5B-RET protein and the suppression of this growth by vandetanib. Representative pictures of colonies without vandetanib treatment (top). Scale bars, 50 μm. Bar graph showing the percentage (± s.d.) of colonies formed after treatment with the indicated amounts of vandetanib (average results of three independent experiments) with respect to those formed by DMSO-treated cells. The study was approved by the institutional review boards of institutions participating in this study.

United States (an individual of European ancestry) (**Supplementary Fig. 7**), but we detected no fusion transcripts in the 34 subjects from Norway (**Supplementary Table 3**); *KIF5B-RET* fusions occurred in 1–2% of LADCs in both Asians and non-Asians. The individual from the United States with the *RET* fusion was classified as an 'ever smoker', whereas the six individuals from Japan with the *RET* fusion were 'never smokers' (**Table 1**). Therefore, prevalence of LADC with regard to smoking status is unclear. We did not detect the *KIF5B-RET* fusion in other major subtypes of lung cancer, including 234 squamous-cell, 17 large-cell and 20 small-cell lung carcinomas (**Supplementary Table 3**). The fusion was also not present in other types of adenocarcinomas, including those of the ovary (n = 100) and colon (n = 200) (data not shown), suggesting that it is specific to LADC.

All seven subjects with LADC harboring the *KIF5B-RET* fusion were negative for *EGFR*, *KRAS* and *ALK* mutations or fusions and were negative for mutations in *HER2*, which is an additional driver mutation in LADC[10] (**Table 1** and **Supplementary Table 4**). The mutually exclusive nature of the *RET* fusions and other oncogenic alterations[1,2,11] suggests that the *KIF5B-RET* fusion is a driver mutation. All proteins encoded by the four *KIF5B-RET* fusion variants contained the KIF5B coiled-coil domain, which functions in protein dimerization[12], and retained the full RET kinase domain, similar to other types of oncogenic *RET* fusions observed in thyroid tumors (**Fig. 1a**)[13]. The KIF5B-RET proteins are likely to form a homodimer through the coiled-coil domain of KIF5B, causing an aberrant activation of the kinase function of RET in a manner similar to the *PTC-RET* and *KIF5B-ALK* fusions[7,14]. In fact, the N-terminal portion of the KIF5B coiled-coil region, which is retained in all variants, has been predicted to have the ability to dimerize through two coiled-coil structures[15]. Consistently, when the *KIF5B-RET* variant 1 was exogenously expressed in H1299 human lung cancer cells without wild-type or fusion *RET* expression, Tyr905, which is located in the activation loop of the RET kinase site[15,16], was phosphorylated in the absence of serum stimulation, indicating an aberrant activation of *RET* kinase[16,17] by fusion with *KIF5B* (**Fig. 1c**). This phosphorylation was suppressed by vandetanib, a TKI against RET (as well as other tyrosine kinases, including EGFR and VEGFR)[18] (**Fig. 1c** and **Supplementary Fig. 8**).

Expression of exogenous *KIF5B-RET*, but not *KIF5B-RET*-KD (a kinase-dead mutant corresponding to S765P in wild-type RET[17]), induced morphological transformation (**Supplementary Fig. 9**) and anchorage-independent growth of NIH3T3 fibroblasts in a way that was analogous to the induction caused by mutant *KRAS* (KRASV12) (**Fig. 1d**). Consistently, phosphorylation of Tyr905 was higher in the KIF5B-RET

Table 1 Characteristics of lung adenocarcinomas with the *KIF5B-RET* fusion

Sample	Country	Sex	Age[a]	Smoking	*KIF5B-RET* fusion[b]	Pathological stage	Pathological findings	RET staining	TTF-1 staining	Napsin A staining	Thyroglobulin staining
BR0020	Japan	Male	57	Never	K15; R12 (variant 1)	IIB	Moderately differentiated ADC	+	+	+	–
BR1001	Japan	Female	65	Never	K15; R12 (variant 1)	IB	Well differentiated ADC	+	+	+	–
BR1002	Japan	Female	64	Never	K15; R12 (variant 1)	IB	Well differentiated ADC	+	+	+	–
BR0030	Japan	Male	57	Never	K16; R12 (variant 2)	IA	Well differentiated ADC	+	+	+	–
BR1003	Japan	Male	28	Never	K23; R12 (variant 3)	IA	Well differentiated ADC	+	+	+	–
BR1004	Japan	Female	71	Never	K24; R8 (variant 4)	IA	Moderately differentiated ADC	NT	NT	NT	NT
NCI1580	USA	Male	63	Ever[c]	K15; R12 (variant 1)	II	Moderately differentiated ADC	NT	NT	NT	NT

[a]Age in years. [b]Fused exon numbers of *KIF5B* (K) and *RET* (R); and variant types (in parentheses) are shown. None of the subjects had oncogenic *EGFR*, *KRAS*, *HER2* or *ALK* mutations or fusions. [c]The number of pack years smoked for this subject is not known. NT, not tested.

protein than in the KIF5B-RET-KD protein. The anchorage-independent growth induced by *KIF5B-RET* was suppressed by treatment with vandetanib (<1 μM), whereas the growth induced by mutant *KRAS* was not (**Fig. 1d**). These results are similar to those observed for *RET* fusions in thyroid cancer[19]. We also detected phosphorylation of the KIF5B-RET protein at Tyr905 in fusion-positive LADC specimens (**Supplementary Fig. 6**). These results suggest that the *RET* fusions are a previously unidentified LADC driver mutation and a potential target for existing TKIs, including vandetanib, which has been recently approved by the US Food and Drug Administration for the treatment of thyroid cancer[18]. Further studies are warranted to promote molecular subtype diagnoses and personalized therapy options for LADC. For this purpose, both the clinical and biological features of this fusion are being investigated. For further information, please see the **Supplementary Note** and **Supplementary Tables 5** and **6**.

Note: Supplementary information is available on the Nature Medicine website.

ACKNOWLEDGMENTS

This work was supported in part by the program for promotion of Fundamental Studies in Health Sciences of the National Institute of Biomedical Innovation (NiBio), Grants-in-Aid from the Ministry of Health, Labour and Welfare for the 3rd-term Comprehensive 10-year Strategy for Cancer Control, the National Cancer Center Research and Development Fund and the Norwegian Cancer Society. National Cancer Center Biobank is supported by the National Cancer Center Research and Development Fund, Japan. We thank T. Urushidate, S. Ohashi, S. Mitani, K. Yokozawa, S. Wakai, C. Otsubo and H. Isomura of the National Cancer Center and D. Suzuki and K. Nagase of the National Center for Global Health and Medicine for technical assistance. We also thank J.D. Minna and L. Girard of the University of Texas Southwestern Medical Center, K. Kumamoto of Saitama Medical University and A. Okamoto of Jikei University for *RET* fusion screening, N. Morii of the National Institute of Advanced Industrial Science and Technology (AIST) for thermodynamic characterization of the KIF5B protein and M. Maekawa of the GSP laboratory for rapid preparation of the FISH probes.

AUTHOR CONTRIBUTIONS

RNA sequencing: H.I., K.Y., M.H., T.N. and H.S. Sequence data processing: Y.T., S.C. and I.Y. Molecular biological analyses: T.K., Y.S., R.I., H. Ogiwara, T.O., M.E., A.J.S., H. Okayama, A.H., Y.A. and S.O. Clinical and pathological analyses: K.T., K.F., V.S., S.W., I.S. and H.T. Manuscript writing: T.K., H.I. and T.S. Study design: T.K., H.I., C.C.H., T.Y., J.Y. and T.S.

COMPETING FINANCIAL INTERESTS

The authors declare no competing financial interests.

Published online at http://www.nature.com/naturemedicine/.
Reprints and permissions information is available online at http://www.nature.com/reprints/index.html.

1. Janku, F., Stewart, D.J. & Kurzrock, R. *Nat. Rev. Clin. Oncol.* **7**, 401–414 (2010).
2. Gerber, D.E. & Minna, J.D. *Cancer Cell* **18**, 548–551 (2010).
3. Lovly, C.M. & Carbone, D.P. *Nat. Rev. Clin. Oncol.* **8**, 68–70 (2011).
4. Soda, M. *et al. Nature* **448**, 561–566 (2007).
5. Meyerson, M., Gabriel, S. & Getz, G. *Nat. Rev. Genet.* **11**, 685–696 (2010).
6. Mani, R.S. & Chinnaiyan, A.M. *Nat. Rev. Genet.* **11**, 819–829 (2010).
7. Wells, S.A. Jr. & Santoro, M. *Clin. Cancer Res.* **15**, 7119–7123 (2009).
8. Bishop, J.A., Sharma, R. & Illei, P.B. *Hum. Pathol.* **41**, 20–25 (2010).
9. DeLellis, R.A., Shin, S.J. & Treaba, D.O. *Immunohistology of Endocrine Tumors* (Saunders, Philadelphia, Pennsylvania, USA, 2010).
10. Shigematsu, H. *et al. Cancer Res.* **65**, 1642–1646 (2005).
11. Herbst, R.S., Heymach, J.V. & Lippman, S.M. *N. Engl. J. Med.* **359**, 1367–1380 (2008).
12. Hirokawa, N., Noda, Y., Tanaka, Y. & Niwa, S. *Nat. Rev. Mol. Cell Biol.* **10**, 682–696 (2009).
13. Jhiang, S.M. *Oncogene* **19**, 5590–5597 (2000).
14. Takeuchi, K. *et al. Clin. Cancer Res.* **15**, 3143–3149 (2009).
15. Morii, H., Takenawa, T., Arisaka, F. & Shimizu, T. *Biochemistry* **36**, 1933–1942 (1997).
16. Vitagliano, D. *et al. Endocr. Relat. Cancer* **18**, 1–11 (2011).
17. Croyle, M. *et al. Cancer Res.* **68**, 4183–4191 (2008).
18. Commander, H., Whiteside, G. & Perry, C. *Drugs* **71**, 1355–1365 (2011).
19. Carlomagno, F. *et al. Cancer Res.* **62**, 7284–7290 (2002).

Lung Cancer 72 (2011) 309–315

Contents lists available at ScienceDirect

Lung Cancer

journal homepage: www.elsevier.com/locate/lungcan

Frequent *ALK* rearrangement and TTF-1/p63 co-expression in lung adenocarcinoma with signet-ring cell component

Akihiko Yoshida[a,b], Koji Tsuta[a], Shun-ichi Watanabe[c], Ikuo Sekine[d], Masashi Fukayama[b], Hitoshi Tsuda[a], Koh Furuta[a], Tatsuhiro Shibata[e,*]

[a] *Clinical Laboratory Division, National Cancer Center Hospital, Japan*
[b] *Department of Pathology, University of Tokyo, Japan*
[c] *Thoracic Surgery Division, National Cancer Center Hospital, Japan*
[d] *Division of Internal Medicine and Thoracic Oncology, National Cancer Center Hospital, Japan*
[e] *Cancer Genomics Project, Center for Medical Genomics, National Cancer Center Research Institute, 5-1-1 Tsukiji, Chuo-ku, Tokyo 104-0045 Japan*

ARTICLE INFO

Article history:
Received 10 June 2010
Received in revised form 9 September 2010
Accepted 19 September 2010

Keywords:
Adenocarcinoma
Signet-ring cell
ALK translocation
Immunohistochemistry
Polymerase chain reaction
Fluorescence in situ hybridization

ABSTRACT

Primary adenocarcinoma with signet-ring cell component (Ad-SRCC) of the lung has been well characterized clinicopathologically and histologically, but their genetics has rarely been investigated. A recent report suggesting an association between Ad-SRCC and *EML4-ALK* fusion prompted us to undertake a histological, immunohistochemical, and molecular analysis of 10 cases of primary Ad-SRCC identified out of 699 lung adenocarcinomas (1.4%). Most of the Ad-SRCCs showed characteristic architectural as well as cytological features including cohesive clustering of signet-ring cells, a solid/acinar growth pattern, and alveolar filling at the tumor periphery. Diffuse co-expression of TTF-1 and p63 was observed in half of the Ad-SRCCs, and this immunoprofile has not been recognized previously. Four Ad-SRCCs (40%) harbored *ALK* translocations detected by reverse-transcriptase polymerase chain reaction, fluorescence in situ hybridization, and immunohistochemistry. One new *EML4-ALK* fusion variant was identified. One *ALK*-rearranged tumor showed focal squamous differentiation. None of the present Ad-SRCCs had *EGFR* or *KRAS* mutations, regardless of *ALK* status. This study successfully utilized tumor histology alone to identify a subset of adenocarcinomas showing a high rate of *ALK* translocation. The characteristic histology, immunoprofile, frequent *ALK* translocation, and total lack of *EGFR* or *KRAS* mutations, may suggest that Ad-SRCC forms a histologically/molecularly coherent subgroup of adenocarcinoma.

1. Introduction

Lung cancer is the leading cause of cancer death both in men and women worldwide. Surgery, chemotherapy, and radiation therapy are the standard therapeutic modalities [1], and the treatment of lung cancer has conventionally been dictated by histological classification and tumor stage [1,2]. In recent years, the classification of lung cancer has become refined by molecular genetic data, and this trend has important therapeutic implications, helping to guide clinicians to the optimal treatment for individual patients [3,4].

In 2007, Soda et al. [5] discovered a novel transforming fusion gene joining the echinoderm microtubule-associated protein-like 4 (*EML4*) and anaplastic lymphoma kinase (*ALK*) genes in a subset of non-small-cell lung carcinoma (NSCLC). The *EML4-ALK* fusion gene is formed by a small inversion within the short arm of chromosome 2, and the encoded protein, a chimera comprising the N-terminal part of EML4 and the intracellular catalytic domain of ALK, is expressed constitutively and dimerized without ligand stimulation [5]. The presence of the *EML4-ALK* fusion in NSCLCs was subsequently confirmed by other investigators worldwide [6–16]. A number of fusion variants have been identified to date, and another rare fusion partner for *ALK* is *KIF5B* [15]. Since ALK is a tyrosine kinase receptor, this subtype of NSCLC is expected to be a good candidate for treatment with small-molecule ALK tyrosine kinase inhibitors [2,17]. Several studies have already confirmed that such drugs induce growth cessation of *ALK*-translocation-positive NSCLC in vitro [5,10] and in xenografts [10,18]. A preliminary phase I study of one of such drugs yielded promising results in a cohort of patients with *ALK*-rearranged NSCLCs [19].

Signet-ring cell component in primary adenocarcinoma of the lung has been recognized for more than two decades [20]. The clinicopathological features of adenocarcinoma with signet-ring cell component (Ad-SRCC) have been well described in the literature [21,22], and its histological features repeatedly documented [21,23–25]. However, the genetic background of this subtype of adenocarcinoma has not been investigated in detail [24,26], and

* Corresponding author. Tel.: +81 3 3547 5201x3123; fax: +81 3 3547 5137.
E-mail address: tashibat@ncc.go.jp (T. Shibata).

0169-5002/$ – see front matter © 2010 Elsevier Ireland Ltd. All rights reserved.
doi:10.1016/j.lungcan.2010.09.013

there has been a paucity of comprehensive analyses of Ad-SRCCs covering both phenotypic and molecular genetic aspects. Recently, Rodig et al. [11] identified frequent signet-ring cell populations in 20 adenocarcinomas that carried *ALK*-rearrangement by fluorescence in situ hybridization (FISH) analysis. Prompted by this report, we examined 10 consecutive cases of surgically resected Ad-SRCCs of the lung. Along with a detailed histological study and standard *EGFR* and *KRAS* mutation assays, we investigated the *ALK* status of these tumors using multiplex reverse-transcription polymerase chain reaction (RT-PCR), FISH, and immunohistochemistry (IHC).

2. Materials and methods

2.1. Case selection

We reviewed 699 consecutive primary adenocarcinomas of the lung resected at the National Cancer Center (NCC), Tokyo, in 2004 and 2005, and retrieved cases of Ad-SRCC. The possibility of metastasis from other sites was clinically/radiologically excluded. The diagnosis of Ad-SRCC was based on the presence of signet-ring cells, which have marginally located crescentic nuclei and abundant intracytoplasmic mucin, the latter being highlighted dark blue by alcian blue- periodic acid-Schiff (AB-PAS) staining. We accepted tumors as Ad-SRCCs when unequivocal signet-ring cells accounted for ≥5% of the total tumor cells. This cutoff is chosen because there is no universally agreed upon threshold, and because routine histological examination can readily identify signet-ring cells when they occupy at least 5% of the tumor cells based on our experience and that of others [27]. The signet-ring cell percentage was calculated after reviewing all the available slides, which represented the entire lesion in small-sized tumors (3.0 cm or less), or the product of adequate sampling in larger tumors. Mucinous bronchioloalveolar carcinoma (BAC), colloid carcinoma, and solid adenocarcinoma with mucin production may contain variably shaped mucus cells [23,28], but they generally lack signet-ring cells ≥5% and are therefore differentiated from Ad-SRCC. Each adenocarcinoma was estimated for tumor size, percentage of signet-ring cells among total tumor cells, nuclear grade (low, intermediate, or high), TNM stage [29], and predominant growth pattern as defined by the World Health Organization (WHO) [1]. Clinical information for each case was collected by reviewing the medical records. This study was approved by the Institutional Review Board of NCC.

2.2. IHC

Four-micrometer-thick sections were deparaffinized. Heat-induced epitope retrieval was performed with 1.0-mmol/L citrate buffer (pH 6.0) for ALK protein and TTF-1, and with TRS9 (DAKO, Carpinteria, CA) for p63. The slides were treated with 3% hydrogen peroxide for 20 min. The slides were then incubated with primary antibodies against ALK protein (1:40, ALK1, DAKO), p63 (1:400, 4A4, DAKO), and TTF-1 (1:100, 8G7G3/1, DAKO) for 1 h at room temperature. Immunoreactions were detected using the Envison-plus system (DAKO) for p63 and TTF-1, and CSAII (DAKO) for ALK protein. The reactions were visualized with 3,3′-diaminobenzidine. Appropriate positive and negative controls were used. Only the nuclear stain was deemed positive for TTF-1 and p63, and the extent of staining was graded as 0 (0–10%), 1+ (>10–25%), 2+ (>25–50%), and 3+ (>50%). Strong diffuse granular cytoplasmic staining was regarded as positive for ALK.

2.3. FISH

FISH was performed on formalin-fixed, paraffin-embedded tumor tissues using a break-apart probe for the *ALK* gene (Vysis LSI ALK Dual Color, break-apart rearrangement probe; Abbott Molecular) in accordance with the manufacturer's instructions. Positive rearrangement was defined as a splitting apart of the fluorescence probes flanking the *ALK* locus. In addition, as recently shown by others in abstract form [30], loss of 5′ locus (green signal) of split-apart *ALK* was considered equivalent to the *ALK* rearrangement, likely reflecting the loss of non-functioning *ALK-EML4* fusion product. Three experienced observers independently assessed the slides. Adjacent uninvolved lung tissue was used as negative control. Decisions regarding positivity and negativity required unanimous agreement among three observers, and cases for which opinions were divided were designated indeterminate for *ALK* rearrangement.

Table 1
Primers used for RT-PCR and sequencing.

For detection of *EML4-ALK* fusion	
EA-F1	5′ GTGCAGTGTTTAGCATTCTTGGGG 3′
EA-F2	5′ AGCTACATCACACACCTTGACTGG 3′
EA-F3	5′ TACCAGTGCTGTCTCAATTGCAGG 3′
EA-F4	5′ GCTTTCCCCGCAAGATGGACGG 3′
ALK-R	5′ TCTTGCCAGCAAAGCAGTAGTTGG 3′
For detection of *KIF5B-ALK* fusion	
KA-F1	5′ CAGCTGAGAGAGTGAAAGCTTTGG 3′
KA-F2	5′ GACAGTTGGAGGAATCTGTCGATG 3′
KA-F3	5′ ATCCTGCGGAACACTATTCAGTGG 3′
KA-F4	5′ TCAAGCACATCTCAAGAGCAAGTG 3′
ALK-R	5′ TCTTGCCAGCAAAGCAGTAGTTGG 3′
For detection of *EGFR* mutation	
EGFR-RTF1	5′ CCTCTTACACCCAGTGGAGAAGC 3′
EGFR-RTR1	5′ CAGTTGAGCAGGTACTGGGAGCC 3′
EGFR-RTF2	5′ TCCTGGACTATGTCCGGGAACAC 3′
EGFR-RTR2	5′ AGGTCATCAACTCCCAAACGGTC 3′
For detection of *KRAS* mutation	
KRAS-RTF1	5′ AGAGAGGCCTGCTGAAAATGACTG 3′
KRAS-RTR1	5′ CCATAGGTACATCTTCAGAGTCC 3′

2.4. RT-PCR and sequencing for ALK fusions

Frozen tumor tissues were powdered by CP02 (Covaris, Woburn, MA) and sonicated using a Covaris S2 (Covaris). Total RNA was extracted using a mirVana RNA Isolation Kit (Ambion, Foster City, CA). cDNA was synthesized with MMTV reverse transcriptase (Transcriptor First Strand cDNA Synthesis Kit, Roche Diagnostics, Switzerland). To amplify *ALK* fusion genes, a mixture of primers covering potential breakpoints of fusion transcripts (*EML4-ALK* and *KIF5B-ALK*, respectively) were used as reported previously (the sequences of the primers used are listed in Table 1) [7,15]. The multiplex PCR conditions were 95 °C for 60 s, followed by 50 cycles of 94 °C for 15 s, 60 C for 30 s, and 72 C for 60 s. The PCR products were electrophoresed, and potential fusion transcripts were purified and sequenced with an ABI 3130 Sequencer using PCR primers (BigDye Terminator v3.1 Cycle Sequencing Kit, Applied Biosystems, Foster City, CA). In addition, the PCR products were subcloned into a TA-cloning vector (Invitrogen, Carlsbad, CA) and sequenced using M13 primers.

2.5. EGFR and KRAS mutation analysis

In cases 1–9, partial cDNAs of the *EGFR* (codon 700–909) and *KRAS* (codon 1–108) genes covering potential mutation hotspots were amplified by RT-PCR and sequenced as described above. The primer sequences are listed in Table 1. Case 10, for which frozen material was not available, was studied by high-resolution melting analysis for the common *EGFR* (L858R mutation and exon 19 deletion) and *KRAS* (codons 12 and 13) alterations, as performed routinely at our institution [31].